THE ASTROPHYSICAL JOURNAL, 295:466–478, 1985 August 15

LARGE-SCALE STRUCTURE OF THE TAURUS MOLECULAR COMPLEX. II. ANALYSIS OF VELOCITY FLUCTUATIONS AND TURBULENCE

STEVEN C. KLEINER AND ROBERT L. DICKMAN
Five College Radio Astronomy Observatory; and Department of Physics and Astronomy, University of Massachusetts
Received 1984 October 18; accepted 1985 February 25

ABSTRACT

The dynamical influence of turbulence within a molecular cloud is determined in part by the degree of correlation between the velocities of nearby gas elements; these are described by the velocity autocorrelation function (ACF). The ACF of observed spectral line centroid fluctuations is shown to reproduce effectively the actual ACF of turbulent gas motions within an interstellar cloud. This provides a framework for study of the large-scale velocity structure of the Taurus dark cloud complex as traced out by our ^{13}CO $J = 1 \rightarrow 0$ observations of this region.

The complex as a whole appears to be in virial equilibrium. Apart from large-scale correlations due to a systematic velocity progression along the central axis of the complex, we find no significant isotropic velocity correlations at smaller scales. Our sample spacing of 15′ (0.6 pc at $D = 140$ pc) therefore serves as an upper limit to the apparent correlation length of turbulent motions within the Taurus molecular system. This result is discussed in the context of recent suggestions that widely observed correlations between molecular line widths and cloud sizes indicate the presence of a continuum of turbulent motions within the dense interstellar medium.

Subject headings: interstellar: molecules — turbulence

I. INTRODUCTION

The existence of turbulence within molecular clouds may have dramatic structural and evolutionary consequences. Turbulent motions provide dynamical support against self-gravity, acting in addition to thermal and magnetic pressures (e.g., Chandrasekhar 1951; Sasao 1971), and the fact that turbulence always possesses one or more spatial coherence lengths (see below) implies that such support is intrinsically scale-dependent. This has potentially important ramifications for the support and fragmentation mechanisms which govern star formation within molecular clouds (Arny 1971; Hunter and Fleck 1982; Roczyczka, Tscharnuter, and Yorke 1980; Fleck 1980). Indeed, the intrinsic nonpredictability associated with turbulent density and velocity fluctuations may render star formation an inherently stochastic process if turbulence turns out to dominate the velocity fields of stellar birth sites; in some respects this would require a considerable shift in current theoretical perspectives. Turbulent transport is highly efficient, entailing important potential consequences for the transport of both material and angular momentum within molecular clouds (e.g., Boland and de Jong 1982; Regev and Shaviv 1981). Finally, turbulence is fundamentally dissipative (e.g., Tennekes and Lumley 1972). If present at the supersonic levels usually suggested by molecular line observations, turbulence must play an exceedingly important role in the energetics of molecular clouds (e.g., Bash, Hausman, and Papaloizou 1981; Franco 1983; Scalo and Pumphrey 1982).

In order to determine fully the dynamical impact of turbulent motions within a physical system, one must have complete knowledge of either (1) both the density and velocity fields, so that one has a well-conditioned initial-value problem subject to appropriate boundary conditions (e.g., Eckmann 1981), or (2) the infinite set of n-order correlation tensors which describe the self-coherence as well as the cross-coherence of the velocity and density fields. The first approach appears to be utterly impractical for the study of interstellar clouds; the second, while associated with a number of theoretical complications—generally termed the "closure problem" (e.g., Leslie 1973)—appears a much more promising avenue for observational exploration.

It is reasonable that the dynamical influence of turbulent motions should depend to a large degree simply upon their magnitude and spatial correlation scale. Turbulence is never completely chaotic: at length scales described by a correlation length λ_c, turbulent motions begin to become coherent and shed their seemingly chaotic behavior. Thus, the character and resulting physical impact of a turbulent velocity field will appear very different at scales much larger than, and much smaller than, λ_c. Determining the correlation scale and amplitude of turbulent gas motions in the interstellar medium is therefore an observational problem of basic importance.

In principle, the correlation length of a turbulent flow may be determined by observing how the average (rms) amplitude of turbulent motions varies with respect to region size. In particular, if the interstellar medium is assumed to be uniformly pervaded by turbulence with correlation length λ_c, then the amplitude of gas motions within a cloud of size L will be an increasing function of L, provided that $L < \lambda_c$; for clouds with $L > \lambda_c$, the internal velocity field reaches a maximum amplitude and then becomes independent of L. Since the width, Δv, of an optically thin molecular line is determined by the velocity distribution of the gas which forms the line, any variation of Δv with L in an ensemble of clouds may reflect, albeit indirectly, the structure of the velocity field within the interstellar medium. This notion has been pursued by Larson (1981) and others, who determined that a correlation between Δv and L apparently does exist for molecular clouds, and who have suggested that it may constitute evidence for a dissipationless cascade of turbulent motions in the interstellar medium (see below and § IV*b*).

This paper adopts a more direct approach to the investigation of turbulence within molecular clouds. It is the second of two which apply autocorrelation techniques to the study of the large-scale structure of the Taurus dark clouds. The first (Kleiner and Dickman 1984, hereafter Paper I) studied the spatial structure of column density fluctuations within the complex and reported a correlation between condensations which may represent a fossil Jeans wavelength frozen into the Taurus clouds. In this work, we use the autocorrelation function of ^{13}CO $J = 1 \rightarrow 0$ spectral line centroid velocity fluctuations to trace the properties of turbulence within the complex. We begin by describing how correlation measures can be used to characterize a turbulent velocity field (§ II), relegating methodological details to a companion paper (Dickman and Kleiner 1985, hereafter Paper III). We then review the observational data which underlie the present study, and we describe the derived velocity correlations on both large and small spatial scales (§ III). Results are discussed in § IV. Although we detect a systematic variation of velocities along the central portions of the Taurus complex, we resolve no significant isotropic correlations of centroid velocity fluctuations on smaller scales. Thus, the 15′ sample spacing of our observations, which corresponds to a scale 0.6 pc (at an assumed distance $D = 140$ pc; Elias 1978) provides an upper limit to the apparent correlation length of turbulence within the Taurus clouds.

We discuss this result critically in the context of suggestions that the widely observed correlations between molecular cloud line widths and sizes may stem from the presence of a "cascade" of turbulent motions in the dense interstellar medium. We note that a model of this type entails a high degree of correlation for gas motions within individual molecular clouds, correlations which should be easily exposed by the centroid velocity techniques developed in the present paper. While the size and internal velocity dispersion which we determine for the Taurus system are in fact consistent with several previously determined size–line-width correlations for molecular clouds, our failure to resolve velocity correlations on scales larger than our 15′ sample spacing indicates that a cascade model of turbulence is inapplicable to the Taurus dark cloud complex. The assumptions which underlie the cascade model may themselves need reconsideration.

II. CHARACTERIZATION OF TURBULENCE

a) *The Autocorrelation Function*

If inertial forces in a fluid flow become much larger than viscous forces, turbulence may set in; the flow acquires a chaotic and unpredictable aspect (e.g., Landau and Lifshitz 1959). However, turbulent motions are usually not completely random, and motions at nearby points may be correlated with one another to some degree. As a result, statistical measures are frequently useful for describing turbulence. Fundamental among these are the velocity autocovariance tensor $c_{ij}(\boldsymbol{\tau})$, and its normalized form, the autocorrelation tensor $C_{ij}(\boldsymbol{\tau})$.[1] Both describe the mean degree of correlation between velocity fluctuations at points spaced by the vector separation, or *lag*, $\boldsymbol{\tau}$. If the velocity field within a molecular cloud is homogeneous (or spatially stationary), that is, if its statistical properties are not a function of position, then the velocity autocovariance tensor is defined as

$$c_{ij}(\boldsymbol{\tau}) = \langle [v_i(\boldsymbol{r}) - \langle v_i(\boldsymbol{r})\rangle_{\boldsymbol{r}}][v_j(\boldsymbol{r}+\boldsymbol{\tau}) - \langle v_j(\boldsymbol{r})\rangle_{\boldsymbol{r}}]\rangle_{\boldsymbol{r}} . \quad (1)$$

(Subscripted angle brackets surrounding a quantity denote the average value of that quantity taken over the subscripted variable.) Note that $c_{ij}(\boldsymbol{\tau})$ is defined in terms of the *fluctuations* of $v_i(\boldsymbol{r})$ and $v_j(\boldsymbol{r})$ about their mean values, rather than in terms of the values of $v_i(\boldsymbol{r})$ and $v_j(\boldsymbol{r})$ themselves. By the definition given in equation (1), $c_{ij}(\boldsymbol{\tau}) = c_{ij}(-\boldsymbol{\tau})$. The autocorrelation tensor

$$C_{ij}(\boldsymbol{\tau}) = c_{ij}(\boldsymbol{\tau})/c_{ij}(0) \quad (2)$$

is a normalized [i.e., $C_{ij}(0) = 1$] form of $c_{ij}(\boldsymbol{\tau})$.

The autocovariance tensor is a basic descriptive tool in studies of turbulent flow. For example, in an incompressible fluid the Reynolds stress tensor, $\rho c_{ij}(0)$, describes the influence of velocity fluctuations on the mean flow (Tennekes and Lumley 1972), and the tensor's trace measures the turbulent energy density of the fluid. This paper will deal almost exclusively with $C_{zz}(\boldsymbol{\tau})$, the longitudinal autocorrelation function (ACF) of line-of-sight velocity fluctuations, and unless otherwise indicated, $C_{zz}(\boldsymbol{\tau})$ will simply be written $C(\boldsymbol{\tau})$. Similarly, the line-of-sight component of gas motions at $\boldsymbol{r}$, $v_z(\boldsymbol{r}) \equiv v_z(x, y, z)$, will be written $v(x, y, z)$.

The mean distance over which the relative degree of coherence between gas motions falls to e^{-1} is referred to as a *correlation length*, λ_c; a turbulent fluid may possess more than one such scale. Over spatial extents much larger than its greatest correlation length, a turbulent velocity field will appear fully random; on scales much smaller than the smallest λ_c, statistical fluctuations essentially vanish.

b) *ACF of Centroid Velocity Fluctuations*

Positional fluctuations in the velocity centroids of spectral lines can be used as a probe of turbulent gas motions within interstellar clouds. This was pointed out some 30 years ago by Kampé de Fériet (1955), and has since been applied by Münch (1958), Kaplan and Klimishin (1964), Baker (1973), and Chièze and Lazareff (1980), among others (see Dickman 1985 for a review). To illustrate the method, we assume a slablike cloud and adopt coordinates such that the $\hat{\boldsymbol{x}}$-$\hat{\boldsymbol{y}}$ plane coincides with the cloud face; the $\hat{\boldsymbol{z}}$-axis is assumed to lie along the line of sight away from the observer. The line-of-sight component of gas motions at a position $\boldsymbol{r} \equiv x\hat{\boldsymbol{x}} + y\hat{\boldsymbol{y}} + z\hat{\boldsymbol{z}}$ within the cloud is denoted as $v(\boldsymbol{r})$, and the intensity of an emission line observed from a position (x, y) on the cloud face at frequency ν is expressed in terms of $T_a(u; x, y)$, the line's antenna temperature at a spectrometer velocity u. If ν_0 is the rest frequency of the observed transition, then u is defined as the Doppler-equivalent velocity offset:

$$u = \left(\frac{\nu_0 - \nu}{\nu_0}\right)c - u_0 . \quad (3)$$

The constant u_0 depends upon the origin of the velocity scale, and is most conveniently chosen so that $u = 0$ corresponds to the mean velocity of the observed cloud. The centroid velocity of the spectral line profile is defined by

$$v_c(x, y) = \frac{\int_{-\infty}^{\infty} T_a(u; x, y)u\,du}{\int_{-\infty}^{\infty} T_a(u; x, y)\,du} . \quad (4)$$

Once an ensemble of line centroids has been obtained by mapping the cloud, the ACF of centroid velocity fluctuations

[1] The subscripts i, j range over the Cartesian coordinates x, y, z. For example, $v_x(\boldsymbol{r})$ denotes the component of the velocity field parallel to the $\hat{\boldsymbol{x}}$-axis at position $\boldsymbol{r} = x\hat{\boldsymbol{x}} + y\hat{\boldsymbol{y}} + z\hat{\boldsymbol{z}}$, and $c_{xx}(\boldsymbol{\tau})$ measures correlations between the velocity components $v_x(\boldsymbol{r})$ and $v_x(\boldsymbol{r}')$ for points $\boldsymbol{r}$ and $\boldsymbol{r}'$ and separated by $\boldsymbol{\tau}$.

can be calculated:

$$C'(\boldsymbol{\tau}') = \frac{\langle v_c(x, y)v_c(x', y')\rangle_{x,y}}{\langle v_c^2(x, y)\rangle_{x,y}}, \quad (5a)$$

where

$$\boldsymbol{\tau}' = (x' - x)\hat{x} + (y' - y)\hat{y}. \quad (5b)$$

Note that in equation (5a) and all following discussion, u_0 in equation (3) has been chosen so that

$$\langle v_c(x, y)\rangle_{x,y} = 0. \quad (5c)$$

The ACF in equation (5a) possesses the symmetry $C'(-\boldsymbol{\tau}') = C'(\boldsymbol{\tau}')$; its argument is the *vector* lag $\boldsymbol{\tau}'$, which represents a directed separation between data points on the face of the cloud. It is extremely important to maintain this vectorial, two-dimensional approach as long as possible: any molecular cloud may contain systematic (and therefore anisotropic) gas motions, and even isotropic turbulence may appear anisotropic on spatial scales which are a significant fraction of the cloud size.

We show in Paper III that for optically thin emission from a homogeneous cloud, $v_c(x, y)$ is simply the average value of gas velocities along the line of sight through (x, y):

$$v_c(x, y) = \langle v(x, y, z)\rangle_z. \quad (6)$$

The effect of this averaging is to reduce the observed magnitude of any velocity fluctuations in the gas. However, the autocorrelation function of equation (5a) is the *ratio* of the magnitude of velocity fluctuations correlated over lag τ to the magnitude of the fluctuations at zero lag. Since both magnitudes are reduced by averaging through the cloud, the centroid velocity ACF may still be a useful estimator of the velocity ACF describing the three-dimensional gas motions within a molecular cloud.

The analysis described in Paper III indicates that for isotropic turbulence this is indeed the case. $C'(\tau')$ is shown to be a weighted average of the true velocity ACF, $C(\tau)$, over all possible lags between points on each of two lines of sight separated by τ'. For a cloud of depth L,

$$C'(\tau') = \frac{\int_0^L [1 - (z/L)]C((z^2 + \tau'^2)^{1/2})dz}{\int_0^L [1 - (z/L)]C(z)dz}. \quad \text{(III-33)}^2$$

The presence of the triangular weighting function $[1 - (z/L)]$, and the fact that $C(\tau)$ will generally be a decreasing function of lag (Lumley 1971), ensure that spacings near τ' contribute most heavily to the average value. Although $C(\tau)$ is usually not reproduced exactly, $C'(\tau')$ will generally preserve the essential features of $C(\tau)$. To illustrate, Figures 1*a*–1*c* show plots of $C(\tau)$ and $C'(\tau')$ evaluated from equation (III-33) for three model autocorrelation functions,

$$C_1(\tau) = e^{-\tau/\lambda_c}, \quad (7)$$

$$C_2(\tau) = 1 - [(e - 1)/e](\tau/\lambda_c)^{2/3}, \quad (8)$$

$$C_3(\tau) = \frac{1}{1 + (e - 1)(\tau/\lambda_c)^2}. \quad (9)$$

In each plot the solid curve presents the exact autocorrelation function, and the dashed curves illustrate the corresponding centroid velocity ACFs which would be observed from clouds 0.1, 1.0, and 10 correlation lengths deep. The broken horizontal line in each figure represents a relative degree of correlation among fluctuations of e^{-1}; the intersections of this line and the autocorrelation functions therefore define both the true and the apparent correlation lengths for each example.

The calculations shown in Figure 1 indicate that, as the depth of the cloud increases, so does the apparent degree of correlation among fluctuations. A correlation length determined from observation of an interstellar cloud may therefore *overestimate* the actual length scale of turbulent motions within the source. However, calculations for very deep clouds ($L > 10^3\lambda_c$) show that even in the worst cases, the apparent correlation length is no more than twice the true λ_c.

c) *Statistical Measures*

Several statistics may be used to characterize the amplitude of the fluctuating velocity field in a turbulent medium, and it is important to distinguish clearly among them. In the case of optically thin emission from a homogeneous cloud, the shape of a molecular line profile is determined by the distribution of gas velocities along the line of sight. In order to relate observable molecular line parameters to the magnitude of gas motions within a molecular cloud, it is convenient to separate the distribution of gas velocities within a cloud into two components: (1) σ_i^2, the mean square fluctuation of gas velocities along individual lines of sight, with respect to the average gas velocity along each line of sight:

$$\sigma_i^2 = \langle [v(\boldsymbol{r}) - \langle v(\boldsymbol{r})\rangle_z]^2\rangle_r; \quad (10a)$$

and (2) σ_c^2, the mean square variation of the line-of-sight average velocities:

$$\sigma_c^2 = \langle [\langle v(\boldsymbol{r})\rangle_z - \langle v(\boldsymbol{r})\rangle_r]^2\rangle_{x,y}. \quad (10b)$$

In Paper III we show how these two measures can be related to the variance of observed centroid velocity fluctuations as well as to the mean line width of an ensemble of molecular line observations. Our results can be summarized as follows. We have already noted that for optically thin radiation from a homogeneous source, the centroid velocity of a line profile observed at position (x, y) on the cloud face is equal to the mean gas velocity along the line of sight: $v_c(x, y) = \langle v(\boldsymbol{r})\rangle_z$. If the origin of the velocity scale of the observations is chosen to coincide with the mean velocity of the cloud, then

$$\sigma_c^2 = \langle v_c^2(x, y)\rangle_{x,y}. \quad (11)$$

In addition, the line's internal squared velocity dispersion may be written

$$\sigma_i^2(x, y) = \frac{\int_{-\infty}^{\infty} T_a(u; x, y)[u - v_c(x, y)]^2 du}{\int_{-\infty}^{\infty} T_a(u; x, y)du}. \quad (12)$$

It is easily shown (Paper III) that the measure σ_i^2, defined in equation (10a) in terms of the magnitude of gas motions within a cloud, is also equal to the mean internal squared velocity dispersion of the line profiles from the cloud:

$$\sigma_i^2 = \langle \sigma_i^2(x, y)\rangle_{x,y}. \quad (13)$$

The dispersion, σ_i, is easily related to the more conventional full width at half-maximum (FWHM) if the line profiles at (x, y) are assumed to be Gaussian in shape:

$$\langle \Delta v_{\rm FWHM}\rangle_{x,y} = (8 \ln 2)^{1/2}\sigma_i. \quad (14)$$

[2] All equations with numbers prefixed by III are taken from Paper III.

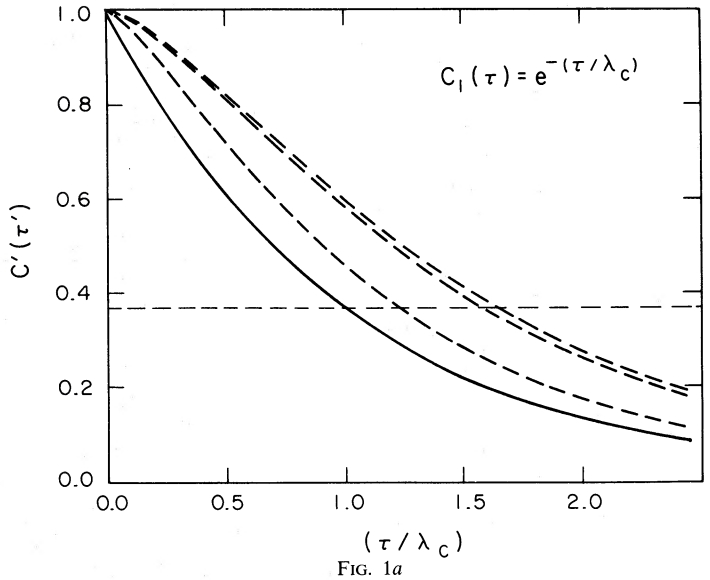

FIG. 1a

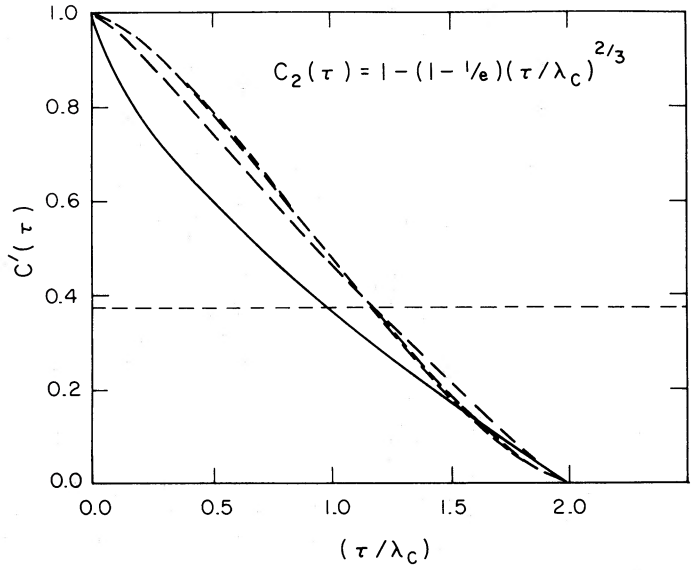

FIG. 1b

FIG. 1.—(*a–c*) Comparison of autocorrelation functions (ACFs) of velocity fluctuations in model molecular clouds [$C(\tau)$ in solid curves], with the ACFs of spectral line centroid velocity fluctuations [$C'(\tau')$ in dashed curves]. Each figure shows $C'(\tau')$ for clouds 0.1, 1.0, and 10.0 correlation lengths deep. The horizontal axis represents lag τ' on the face of the cloud in units of the correlation length λ_c, while the vertical scale indicates the relative degree of correlation. The broken horizontal line is drawn across each figure at e^{-1}. The intersections of this line with the solid and dashed curves define the actual and apparent correlation lengths of the turbulent gas motions in the models. As the cloud depth increases, the curves $C'(\tau')$ move upward and outward from $C(\tau)$, and the apparent correlation length increases. These figures were obtained by evaluating eq. (III-33) for the sample ACFs given by eqs. (7)–(9) in § II*b*.

Together σ_i^2 and σ_c^2 determine an additional measure, σ_p^2, the total or *parent* variance of gas velocities:

$$\sigma_p^2 = \langle [v(\boldsymbol{r}) - \langle v(\boldsymbol{r}) \rangle_r]^2 \rangle_r , \qquad \text{(III-16)}$$

for which it is easily shown that

$$\sigma_p^2 = \sigma_i^2 + \sigma_c^2 . \qquad \text{(III-19)}$$

III. OBSERVATIONS AND DATA ANALYSIS

The data for this paper consist of ~1200 spectra in the $J = 1$–0 transition of ^{13}CO, taken at 15′ spacing and covering the central 8° × 14° region of the Taurus complex. The observations, centered at $\alpha = 4^h30^m$, $\delta = +27°$ ($l_{II} \sim 175°$, $b_{II} \sim -15°$), encompass the areas of contiguous heavy obscuration visible on the Palomar Sky Survey plates which are cataloged by Lynds (1962) as cloud association 169. The observations were made during 1982 June with the 14 m antenna of the Five College Radio Astronomy Observatory,[3] in New Salem, Massachusetts. We adopt a distance to the complex of $D = 140$ pc (Elias 1978), so that the ~50″ angular resolution of the antenna corresponds to a projected spot size of ~0.03 pc; our 15′ map spacing corresponds to a separation of ~0.6 pc between data points. Use of a 256 channel × 100 kHz filter

[3] The FCRAO is operated with support from the National Science Foundation under grant AST 82-12252 and with permission of the Metropolitan District Commission of the Commonwealth of Massachusetts.

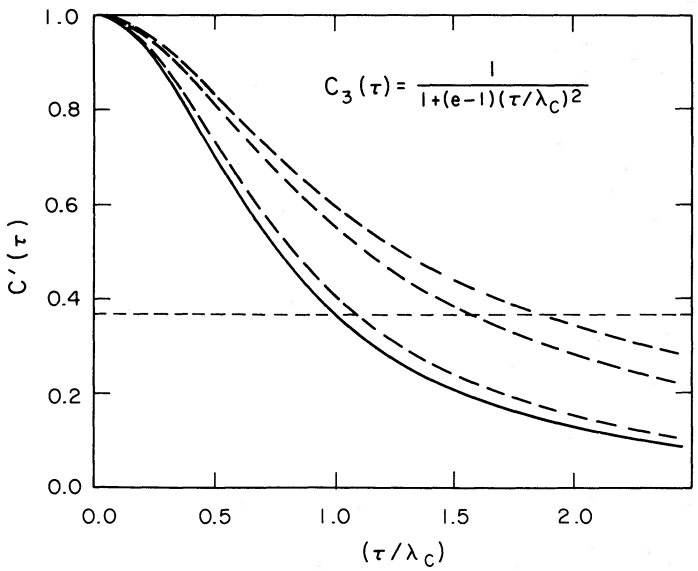

FIG. 1c

bank yielded a velocity resolution of 0.27 km s^{-1}. Further details of the observations are reported in Paper I.

a) Statistical Measures for the Data

We denote the velocity assigned to the center of spectrometer channel i by u_i, and the antenna temperature in that channel due to emission from point (x, y) on the cloud as $T_i(x, y)$. The centroid velocity of the spectral line from (x, y) is calculated as

$$v_c(x, y) = \frac{\sum_{i=1}^{N} u_i T_i(x, y)}{\sum_{i=1}^{N} T_i(x, y)} . \quad (15)$$

The range of N velocity channels used to calculate centroid velocities (which we term the velocity window) need not include all channels available in the spectrometer. Indeed, as discussed in Paper III, smaller windows tend to minimize the effects of instrumental noise. If the window is *too* small, however, real data representing gas motions at velocities far from the mean may be inadvertently discarded. In choosing a window for the Taurus data, we were guided by an ensemble spectral profile consisting of the average of all individual spectra. If the observed molecular emission is not heavily saturated—as expected for ^{13}CO—the ensemble envelope reproduces well the distribution of gas velocities within the complex.

The average profile was reasonably well described by a Gaussian distribution of the form $\exp[-(u - u_0)^2/(2\sigma^2)]$, with $u_0 = 6.4$ km s^{-1} and $\sigma = 0.99$ km s^{-1}. A natural choice for a velocity window would thus have been one $6\ \sigma \sim 6$ km s^{-1} wide. However, a secondary emission component in the line profiles was noted around 4 km s^{-1}. This component was clearly distinct from the bulk of the emission originating from the Taurus complex; therefore, a narrower window, 5.2 km s^{-1} wide, was chosen in order to exclude this extraneous emission.

Within this window the dispersion of centroid velocities was found to be $\sigma_c' = 1.02$ km s^{-1}. Some fraction of σ_c' represents spurious velocity fluctuations induced by instrumental noise. As discussed in Paper III, the magnitude of these fluctuations, σ_n, depends upon the size of the velocity window, the magnitude of instrumental noise, and the intensity of the observed molecular emission. Both numerical simulations and evaluation of equation (III-67) lead to the result $\sigma_n \approx 0.57$ km s^{-1}. Since noise-induced fluctuations are random and independent of the true centroid velocities, the dispersion of centroid velocities, corrected for noise, is

$$\sigma_c = (\sigma_c'^2 - \sigma_n^2)^{1/2} = 0.84 \text{ km s}^{-1} . \quad (16)$$

Let us next consider the dispersion obtained from calculating the ensemble-averaged line width, $\langle \sigma_i(x, y) \rangle_{x,y}$ (§ II). For a discretely sampled spectral line equation (III-20) becomes

$$\sigma_i^2(x, y) = \frac{\sum_{i=1}^{N} T_i(x, y)[u_i - v_c(x, y)]^2}{\sum_{i=1}^{N} T_i(x, y)} . \quad (17)$$

The factor $[u - v_c(x, y)]^2$ which appears in the numerator of equation (17) makes this manner of calculating $\sigma_i^2(x, y)$ very sensitive to noise in $T_i(x, y)$. Numerical simulations indicate that for our data $\sigma_i(x, y)$ may be estimated more reliably from the line's full width at half-intensity:

$$\sigma_i(x, y) \approx \frac{\sum_{i=1}^{N} T_i(x, y)\delta u}{(2\pi)^{1/2} T_{\text{peak}}} . \quad (18)$$

Here δu is the velocity resolution of the spectrometer, T_{peak} is the maximum antenna temperature across the line profile, and a Gaussian line profile has been assumed. While uncertainties result from the application of equation (18) because line profiles are often not Gaussian and because spectrometer resolution limitations made the determination of T_{peak} imprecise, for data with only moderate signal-to-noise ratio this approximation is less sensitive to instrumental noise than is equation (17). Accordingly, we have used it to determine σ_i, and we find that $\sigma_i = 0.48$ km s^{-1}. The parent dispersion of gas motions within the Taurus complex is thus $\sigma_p^2 = \sigma_c^2 + \sigma_i^2 = 0.97$ km s^{-1}. By comparison, σ_p can also be inferred from the ensemble average of the individual profiles, and, as noted already, this value is $\sigma = 0.99$ km s^{-1}. The very small discrepancy between the two determinations is within the uncertainties expected for the instrumental noise correction and with our use of the approximation (18) for σ_i.

b) Autocorrelation of the Data

The mean cloud velocity, $\langle v_c(x, y)\rangle_{x,y}$ was first subtracted from each calculated centroid, and two-dimensional autocorrelation functions of the resulting fluctuation map were computed by Fourier transforming the data power spectrum using standard fast transform routines (e.g., Brenner 1976). When considering velocity correlations in a molecular cloud of finite extent, it is important to distinguish between correlations appearing at small and at large lags. Results at separations small compared with the size of the cloud are formed from the average of a relatively large number of data pairs. These results are statistically the most reliable and probe well the intrinsic nature of the velocity field: the number of sample pairs is large enough that only statistically significant correlations remain in the ACF.

The ACF is also sensitive to structure in gas motions at large scales. However, since the number of data pairs which can be formed at large lags is limited, the ACF cannot distinguish between physically significant systematic motions and anistropic, large-scale statistical fluctuations. Therefore, although the ACF is a useful indicator for the presence of systematic motions within a molecular cloud, the physical importance of correlations seen at large lags must be evaluated independently of their presence in a correlation function.

In Paper I several different estimators for the autocorrelation function of a finite data set were described. In this work we have chosen to employ a *biased* autocorrelation estimator (cf. Paper I); although it underestimates the magnitude of correlations at large lags (where any ACF is noisiest), it is statistically the most trustworthy. The resulting autocorrelation function for the Taurus complex is plotted in Figure 2. Contours indicate the degree of correlation as a function of the vector lag τ (measured from the origin $\tau = 0$, marked by a small cross), and range from -0.15 to 0.65 in steps of 0.05. Dashed contours indicate negative correlations. The symmetry of the plot with respect to inversion through $\tau = 0$—common to all ACFs—is evident.

The ACF presented in Figure 2 has been renormalized after smoothing to have a value of unity at zero lag (although contours between 0.65 and 1.00 are not plotted). The width of the peak at zero lag has been exaggerated by the smoothing process. The smoothing routine used (which is applied to all the correlation surfaces and maps presented in this series of papers in order to improve their legibility) is essentially a low-pass filter; thus, information describing small-scale fluctuations in the data is discarded or suppressed, and the presence of large-scale, systematic variations is emphasized.

c) Structure at Large Lags

The extended correlations seen in Figure 2 along the north-south axis, and the corresponding anticorrelations perpendicular to that direction, indicate the presence of a systematic velocity component, with the pattern of positive and negative correlations suggesting a gradient; motions along the gradient vary most rapidly and soon decorrelate, while those perpendicular to the gradient remain unchanged. Indeed, examination of the map of centroid fluctuations reveals a shift across the central core of the complex, with lower (recession) velocities seen toward center and southwest, and higher velocities toward the northwest. It should be noted, however, that the two condensations east of Heiles 2 (at around $\alpha = 4^h54^m$, $\delta = +26°$; cf. Fig. 1 in Paper I) do *not* share this velocity trend. Therefore, it

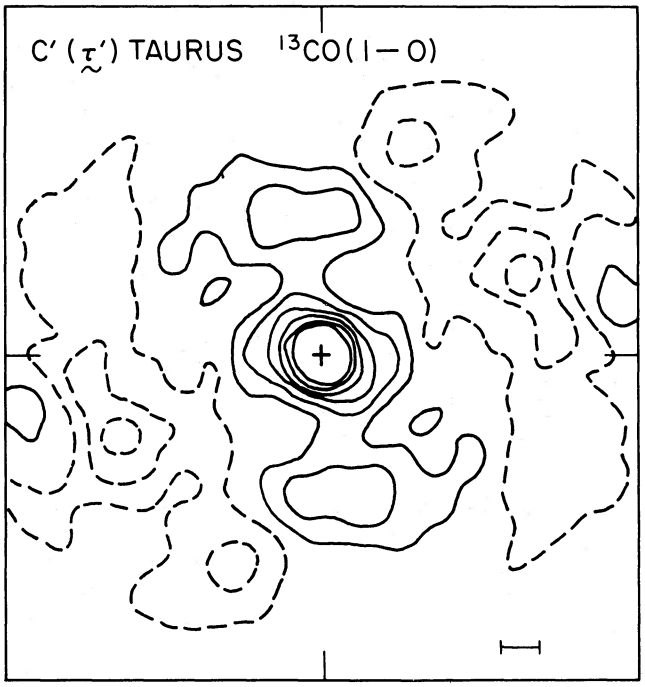

FIG. 2.—The two-dimensional, biased autocorrelation function of ^{13}CO $J = 1 \rightarrow 0$ spectral line centroid velocity fluctuations for the Taurus dark clouds. Contours display the relative degree of correlation of the (smoothed) ACF as a function of vector offset from the origin (marked by a small cross), and range from -0.15 to 0.40 in steps of 0.05. Lags in declination run vertically, and those in right ascension horizontally. The horizontal scale marker in the lower right-hand corner of the figure is 1° long. Thus, for example, contour values along the vertical line through the origin describe the degree of correlation between pairs of observations with the same right ascension, i.e., τ' pointing due north or south. The pattern of correlations extending north and south, and the anticorrelations running east-west, suggest the presence of a velocity gradient in the inner parts of the cloud complex.

is unsurprising that we were unable to find a statistically significant least-squares fit to a model velocity gradient across the data set: a gradient which fits the velocity shift across the core of the complex would not be able to reproduce the centroid velocities of the easternmost condensations.

Centroid velocities, however, may not in any case be the best tracers of *mass* motions within an inhomogeneous cloud. In Paper III we derive a general expression for the velocity centroid of an optically thin line profile when the gas velocity, excitation temperature, and absorption coefficient all vary along the line formation path:

$$v_c(x, y) = \frac{\int_0^L v(\mathbf{r}) T_x(\mathbf{r}) \kappa_0(\mathbf{r}) dz}{\int_0^L T_x(\mathbf{r}) \kappa_0(\mathbf{r}) dz} . \qquad \text{(III-13)}$$

When T_x and κ_0 are both constant everywhere, equation (6) is obtained. More generally, if $T_x(\mathbf{r})$ alone is constant, then since $\kappa_0(\mathbf{r})$ is proportional to the gas density, $\rho(\mathbf{r})$:

$$v_c(x, y) = \frac{\int_0^L v(\mathbf{r}) \rho(\mathbf{r}) dz}{\int_0^L \rho(\mathbf{r}) dz} . \qquad (19)$$

Thus, in a uniformly excited but inhomogeneous cloud, the density weighting of the velocity field in the numerator of expression (19) is strongly suppressed by the column density

term which occurs in the denominator. In order to consider mass motions more directly, therefore, we may examine the quantity $[\sum T_i(x, y)\delta u]v_c(x, y)$ alone. The bracketed term is simply the integrated ^{13}CO antenna temperature, which for optically thin emission is proportional to H_2 column density (Dickman 1978). Thus, $[\sum T_i(x, y)\delta u]v_c(x, y)$ is, in a sense, a tracer of momentum rather than velocity fluctuations. We find that velocity shifts across the cloud core are more conspicuous when viewed in a map of this parameter.

As an additional means of tracing mass motions within the Taurus complex, we consider maps of ^{13}CO emission integrated over narrow velocity intervals. As the centers of these intervals range from lower to higher velocities, the regions of maximum emission from the core shift from the southeast to the northwest, as shown in Figure 3. This corresponds to a velocity shift of ~ 3 km s^{-1}, from 5 to 8 km s^{-1} with respect to the local standard of rest, over a projected distance of 12 pc. Note that the outermost portions of the complex, which are traced by the lowest contours of the maps in Figure 3, do not participate in the velocity progression, suggesting that they do not share the core's apparent rotation. The structure of the core and the dynamical consequences of the velocity shift seen across it will be discussed further in § IV.

d) Structure at Small Lags

Figure 2 suggests that at lags ≤ 3 pc the correlation structure of the Taurus velocity field is approximately isotropic. In Figure 4*a* we discard entirely the angular content of the correlation function and plot values of $C'(\tau')$ versus $|\tau'|$ for $0 \leq |\tau'| \leq 7.2$ pc. (The dashed line in the figure is discussed below.) Two corrections to this raw ACF should be considered before any conclusions are drawn about its shape at small lags. First, radiometer noise in the data causes random centroid velocity fluctuations which reduce the apparent magnitude of any correlations in the data (Paper III). If $C^*(\tau')$ denotes the ACF of centroid velocity fluctuations which would be observed in the absence of instrumental noise, the degradation of the observed ACF at nonzero lags is given by

$$\frac{C'(\tau')}{C^*(\tau')} = 1 - \left(\frac{\sigma_n}{\sigma_c'}\right)^2, \quad \tau' \neq 0 . \qquad \text{(III-41)}$$

Here $\sigma_c'^2$ is the observed variance of centroid velocity fluctuations (*including* those induced by noise), while σ_n^2 is the magnitude of noise-induced fluctuations alone. In § III*a* we noted that $\sigma_c' = 1.02$ km s^{-1} and $\sigma_n = 0.57$ km s^{-1}, so that the correction factor is $C^*(\tau')/C'(\tau') = 1.45$.

The second correction to the autocorrelation function shown in Figure 4*a* is geometrical. As discussed in Paper I, the orientation of the Taurus complex with respect to the plane of the sky may require distances measured along the major axis of the complex to be adjusted for foreshortening. The resulting correction is of the form $[1 + \cos \phi/\cos \theta]$, where θ is the inclination of the major axis of the complex with respect to the plane of the sky and ϕ is the angle between τ and the major axis. As in Paper I, we adopt a value $\theta = 60°$ in calculating this correction. Figure 4*b* is the ACF of Figure 4*a* after correction for instrumental noise and foreshortening.

The fact that the number of data pairs at a given lag is limited in a finite data set may introduce statistical noise into the ACF; random fluctuations within the data may not have the opportunity to average out to a negligible value. To investi-

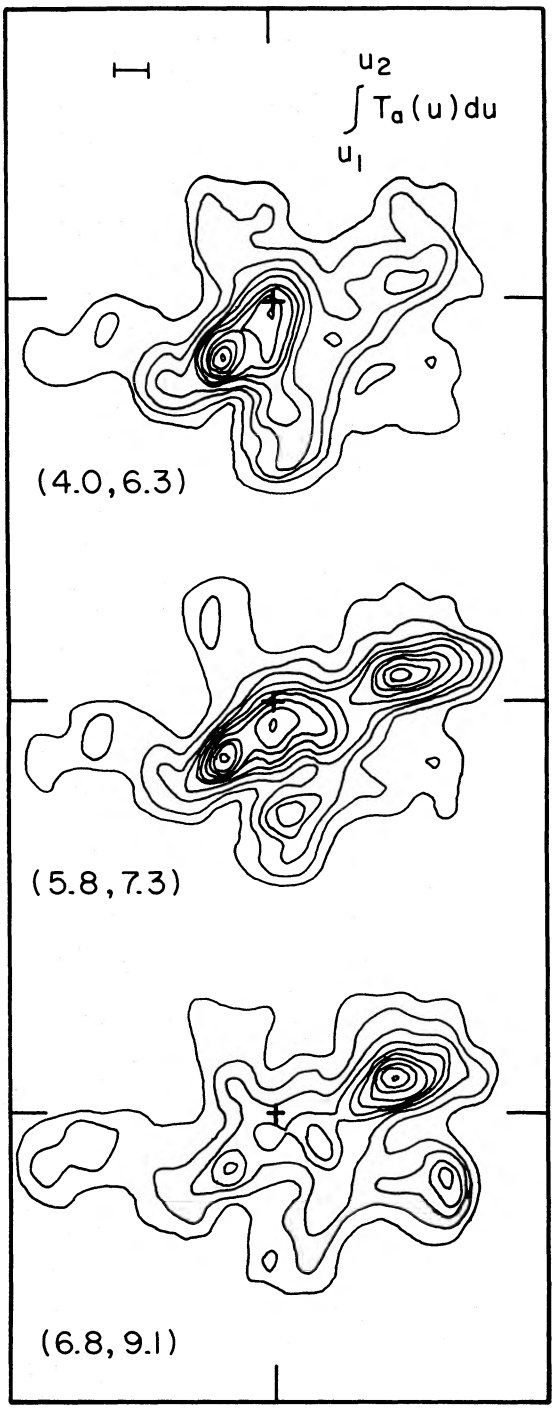

FIG. 3.—Integrated ^{13}CO $J = 1 \rightarrow 0$ antenna temperature over each of three (overlapping) velocity intervals. The limits of integration for each velocity interval (in km s^{-1}) are given in the lower left-hand side of each panel. Right ascension increases to the left, declination toward the top, and the center of each diagram (marked by a small cross) is at $\alpha = 4^h30^m$, $\delta = +27.0$ (1950). The scale marker in the upper left-hand corner is 1° long (2.4 pc at $D = 140$ pc). The shift of regions of peak emission along the core of the complex with increasing velocity is clearly visible. This systematic progression is consistent with the large-scale correlation structure seen in Fig. 2, and may indicate the presence of rotation in the interior regions of the Taurus system. Note, however, that the outermost portions of the complex, traced by the lowest contours of integrated antenna temperature, *do not* appear to share this motion (§ III).

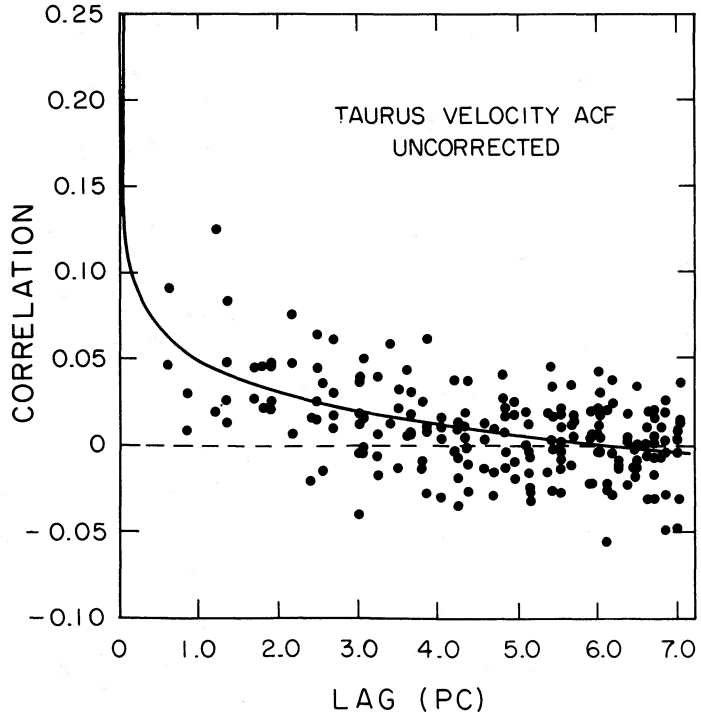

FIG. 4*a*

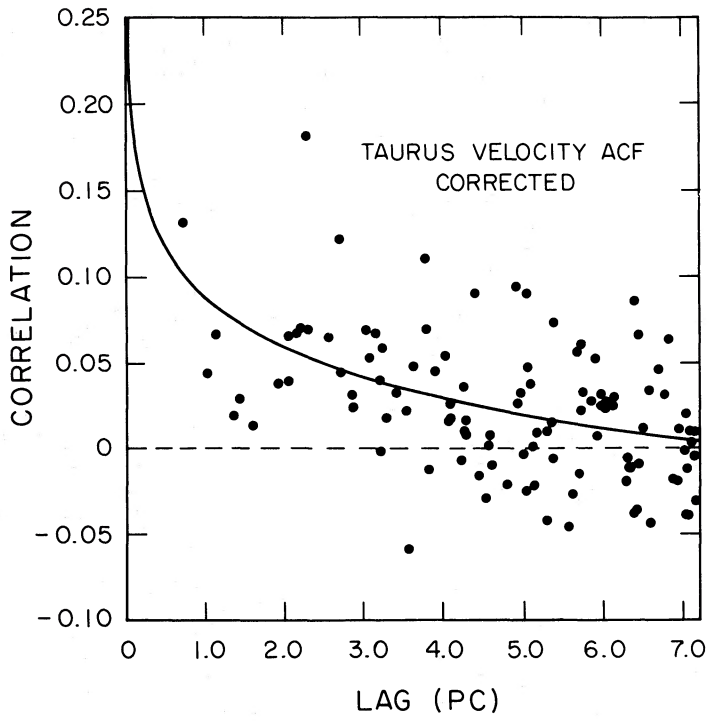

FIG. 4*b*

FIG. 4.—Plots of $C'(\tau')$, the unsmoothed, biased centroid velocity ACF for $0 \leq \tau' \leq 7.2$ pc. Angular information has been discarded in order to investigate the isotropic behavior of velocity correlations at small lags. The dashed curve is the best least-squares fit of $1 - \alpha\tau'^{\beta}$ to the data. Although the data and the fitted curve suggest the presence of some velocity correlation at small lags, no scale length for them is resolved at the e^{-1} level. (*a*) Raw velocity ACF. (*b*) ACF after correcting for the effects of radiometer noise and geometrical foreshortening. (*c*) Comparison ACF of a completely uncorrelated velocity field having the same spatial sampling as the observational data for this paper. The field was generated by replacing the centroid velocity observed at each location in the Taurus complex with a random variable chosen from a normally distributed sample.

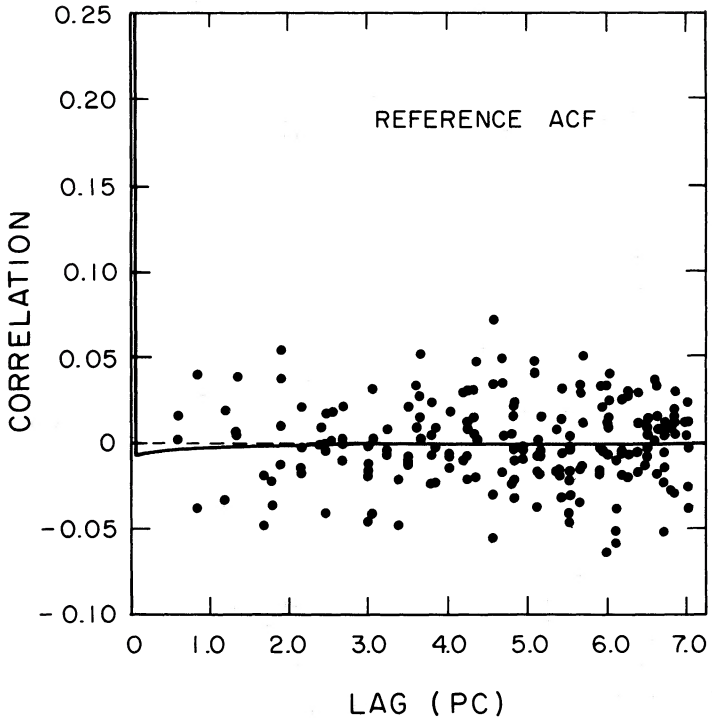

FIG. 4c

gate the effect of the finite and somewhat irregular extent of the Taurus data set, we calculated the ACF of a completely uncorrelated model velocity field having the same spatial distribution as our data. (The model was constructed by setting the centroid velocity at each position observed in Taurus equal to a random value chosen from a Gaussian distribution.) The resulting autocorrelation function is plotted in Figure 4*c* and shows that for the 0–7 pc lags under consideration here, the size of our data set does not introduce significant noise; the ACF drops very rapidly at nonzero lags.

Comparison of Figures 4*a* and 4*b* with Figure 4*c* suggests the presence of some degree of velocity correlation at small lags. In neither case, however, is it obvious that the associated correlation length has been resolved. To further explore the structure of the flow at small separations, and to interpolate the ACF across the e^{-1} line (thus determining the value of the correlation length), we fit model autocorrelation functions to the points shown in Figures 4*a* and 4*b*. Although attempts to fit Gaussian and parabolic model AFCs were unsuccessful, we were able to fit the data with a model power-law function of the form $1 - \alpha\tau^{\beta}$ (shown by the dashed curves in Figs. 4*a* and 4*b*). While this suggests the probable existence of velocity correlations at small lags in the data, correlation lengths obtained in the fits were so much smaller than the sample spacing that we cannot attribute any physical significance to them. We therefore conclude that although there is evidence for correlations between gas motions at small scales within the Taurus complex, their characteristic length remains unresolved in the present data. An upper limit to the correlation length of turbulence within the Taurus molecular cloud complex is therefore the sample spacing of 0.6 pc (assuming a distance to the complex of $D = 140$ pc). In a subsequent paper (Kleiner and Dickman 1985) we analyze the velocity field of the TMC-1 region of the Taurus clouds using data sampled at much smaller (1′) spacings, and we resolve correlation structure at scales consistent with the present upper limit.

As a final matter, the presence of large-scale motions, such as those described in § III*c*, may affect the shape of an autocorrelation function at small lags. Hence, if correlations are observed within a source at small lags—in contrast to the present case—one is obliged to determine whether they reflect intrinsic, small-scale velocity structure, or whether they are merely an artifact of the systematic motions. In general, one may deal with the presence of systematic variations in the data (often termed "trends" or "nonstationary" components) by explicitly identifying and removing them by least-squares fitting, or by using a digital high-pass filter to suppress them (cf. § II, Paper I).

IV. DISCUSSION

a) Core Velocity Gradient and Virial Equilibrium of Complex

Centroid velocities observed along the core of the Taurus complex vary from ~ 5 to 8 km s^{-1} over a projected distance of 12 pc, a gradient of 0.25 km s^{-1} pc^{-1}. If interpreted as a rotation, these values correspond to an angular velocity $\omega = 8.1 \times 10^{-15}$ s^{-1}, in a sense retrograde to Galactic circular motion. The rotation axis points toward the northeast inclined at $\sim 25°$ to the disk of the Galaxy. Viewed in integrated ^{13}CO emission (cf. Fig. 1 of Paper I), the main component of the core is a fragmented lane, less dense toward the middle than at the edges. Its appearance suggests a bar or a thick torus seen edge-on, rather than a disk or coincidentally aligned condensations. The lane stretches from the dark cloud B14 (which includes Heiles 2 and TMC-1) in the southeast, to the B7 complex in the northwest (Barnard 1927). The main com-

ponent is paralleled by a second, less massive, filament to the south, running from B18 (the site of TMC-2) to B208. Together, they resemble a pair of aligned filaments or fragments of a squat, hollow cylinder.

If the centroid velocity shift along the core is taken as evidence of rotation, assessment of the virial equilibrium of the complex must include the rotational energy of the core as well as the kinetic energy of random gas motions. We use M_t to denote the total mass of the complex, and M_r to indicate the mass taking part in the apparently ordered rotation of the core. The maps of integrated ^{13}CO emission and centroid velocity variations suggest that $M_r \sim 0.5M_t$. Twice the rotational energy of the core is $2\mathrm{KE}_r = I\omega^2$, where the moment of inertia of the core is $I = \alpha_g M_r S^2$. S denotes the half-extent of the core along its major axis ($\sim$6 pc), while α_g, $1/12 \leq \alpha_g \leq 1/2$, depends on the distribution of mass within the core (e.g., $\alpha_g = 1/12$ if the core is a bar of gas, or $\alpha_g = 1/2$ if the core is a disk). Two geometrical effects will make $2\mathrm{KE}_r$ inferred from observed values of S and ω a lower limit to the actual rotational kinetic energy of the core. If the plane of rotation of the core is not seen edge-on, ω will be underestimated; and if the core is not parallel to the plane of the sky, the observed value of S will be a lower limit to the actual size of the core. We estimate that

$$2\mathrm{KE}_r = \alpha_g M_r S^2\omega^2 \geq \alpha_g(2.5 \times 10^{47})(M_r/M_t) \text{ ergs} . \quad (20)$$

Is the core gravitationally bound? If v_e is the equatorial velocity of the core ($v_e \sim 1.5$ km s^{-1}), then the mass of the core must exceed $M_r \geq (Sv_e^2)/G$ in order to balance centrifugal and gravitational forces. The sense of the inequality is set by the uncertainties in S and of the core geometry and requires $M_r \geq 3100\ M_\odot$. Since $M_r \sim 0.5M_t$, and $M_t \sim 6000\ M_\odot$ (cf. Paper I), the core thus appears to be marginally bound.

In order to evaluate the overall virial stability of the complex, we shall adopt as a criterion the condition $2\mathrm{KE} + W_g = 0$, where KE and W_g are respectively the kinetic and gravitational potential energies of the complex. This implicitly requires that, excluding the systematic motion of the core, the kinetic energy of the cloud system be due to random, i.e., turbulent, gas motions; this appears reasonable, since the presence of ordered systematic collapse, expansion, or oscillation of the molecular complex *solely* along the line of sight—the only other dynamical possibilities consistent with the absence of a resolved correlation signature in our data—would be an extraordinary coincidence, particularly given the somewhat irregular geometry of the clouds involved.

The irregular geometry of the Taurus clouds complicates determination of their binding energy. Although the extended, filamentary structure of the complex suggests that it be modeled as a section of an infinite cylinder, there is no obvious choice for the radius R_t, describing the transverse extent of the clouds. In Paper I we avoided this issue by reversing the question: assuming a cylindrical, homogeneous cloud supported by internal gas motions, we derived a corresponding equilibrium radius, R_e. Inspection of the ^{13}CO emission map then indicated that R_e fell between the radii of the dense inner core of the complex and that of the more diffuse surrounding gas. We concluded that the observed dimensions, mass, and magnitude of gas motions within the Taurus clouds were consistent with a state of virial equilibrium. A more precise estimate of the stability of the complex, however, requires a specific value for R_t.

Our determination of R_t attempts to account for the inhomogeneous structure of the clouds. We take R_t as the rms transverse extent of the complex weighted by the ^{13}CO column density at (x, y), $N(x, y)$:

$$R_t^2 = \frac{\langle N(x, y)R^2(x, y)\rangle_{x,y}}{\langle N(x, y)\rangle_{x,y}} . \quad (21)$$

Here, $R(x, y)$ is the perpendicular distance from (x, y) to the major axis of the complex. The major axis, in turn, is determined by the requirement that $\sum N(x, y)R^2(x, y)$ be a minimum. Under these conditions, we find that $R_t = 4.0$ pc. The gravitational potential energy of a section of an infinite cylinder is $W_g = -(\frac{2}{3})(GM_t^2/R_t)$. The mass of the complex inferred from integrated ^{13}CO emission (Paper I) is 5700 $M_\odot$, and we find

$$W_{\mathrm{grav}} = -(\tfrac{2}{3})(GM_t^2/R_t) \approx 4.7 \times 10^{47} \text{ ergs} . \quad (22)$$

The kinetic energy of random gas motions within the complex is

$$2\mathrm{KE}_{\mathrm{turb}} = \int \rho(3\sigma_p^2)dV \approx (3.3 \times 10^{47})(1 - M_r/M_t) \text{ ergs} . \quad (23)$$

(The factor 3 in the integrand enters because σ_p^2 measures the variance of gas motions only along the [one-dimensional] line of sight, and we assume that the gas motions are isotropic.) The rotational kinetic energy of the core, calculated above, is

$$2\mathrm{KE}_{\mathrm{rot}} = \alpha_g M_r S^2\omega^2 \geq \alpha_g(2.5 \times 10^{47})(M_r/M_t) \text{ ergs} , \quad (24a)$$

$$1/12 \leq \alpha_g < 1/2 , \quad (24b)$$

so that equations (22)–(24b) indicate that $2\mathrm{KE}_{\mathrm{turb}} + 2\mathrm{KE}_{\mathrm{rot}} \sim -W_{\mathrm{grav}}$, regardless of the value of M_r. Given the uncertainties introduced by the irregular structure of the complex, no better agreement between 2KE and $-W_g$ can be expected, and it thus appears that the Taurus clouds are in virial equilibrium on scales larger than 0.6 pc.

b) Small-Scale Correlation Structure and Turbulence in the Interstellar Medium

We concluded in § III*c* that apart from the apparent rotation exhibited by its core, the Taurus complex possesses gas motions which are essentially uncorrelated on scales larger than 0.6 pc. We now discuss this result in the context of recent studies which have attempted to draw conclusions regarding the characteristics of turbulence in the dense interstellar medium by correlating molecular cloud sizes (L) with internal velocity dispersions (Δv). Let us first summarize the results of these studies.

In 1981, Larson assembled published values of Δv and L for some 60 molecular clouds having sizes in the range $0.5 \leq L \leq 60$ pc, and found a reasonably good correlation in the data of the form $\Delta v \propto L^\beta$, with $\beta = 0.38$. This result was consistent with an earlier compilation (Larson 1979), which also included dispersion velocities and sizes for atomic gas clouds, and for which a similar relation with $\beta \sim \frac{1}{3}$ was determined for length scales ranging to nearly 1 kpc. From observations of a dozen isolated dark globules, Leung, Kutner, and Mead (1982) found a similar power law, but with an index $\beta = 0.48$. Myers (1983) reported a similar index, $\beta = 0.50$, based upon observations of 43 small dark clouds. The scatter in all of these studies is appreciable, and the index β therefore not particularly well established; in part, this is clearly attributable to difficulties in determining reliable cloud distances, but, as suggested by Leung, Kutner, and Mead, it may also reflect a

diversity in source conditions such as kinetic temperature. In any case, using the total velocity dispersion measured for the Taurus complex (0.99 km s^{-1}), along with the region size ($2R \sim 8$ pc) inferred above, leads to a $\Delta v/L$ ratio for this large molecular system consistent with the compilations of both Larson (1979) and Leung, Kutner, and Mead (1982).

Although the specific slope of the Δv-L relation is somewhat uncertain, the existence of a general velocity-size correlation for molecular clouds hardly appears to be in doubt. Unfortunately, its meaning is far less clear. Larson (1981) has argued that the existence of a widespread, scale-invariant correlation of this sort may indicate that gas velocities in the dense interstellar medium stem from a common hierarchy of turbulent motions. In making this suggestion, Larson emphasized that the power-law index of 0.38 for his sample is close to the value of $\frac{1}{3}$ which might be expected to characterize an incompressible, dissipationless turbulent cascade. Models of such cascades, which are sometimes termed "inertial range" turbulence, were first introduced theoretically in 1941 by Kolmogorov and by Obukhov (see Friedlander and Topper 1961). They have the property that energy is presumed to enter the flow at an "outer" scale, λ_o, and to be dissipated solely by molecular viscosity at much smaller dimensions, specified by an "inner" scale, λ_i. The cascade is assumed to be characterized by a unique energy transfer rate, ϵ, per unit mass, which is set by the rate at which kinetic energy can be dissipated at the scale λ_i. If the flow is incompressible and if there are no sources or sinks of energy between the outer and inner scales, one expects the dissipation rate for turbulent motions on intermediate scales l, $\sim v^3(l)/l$, to be independent of l and equal to ϵ. This leads to the prediction $v \propto l^{1/3}$, a result generally known as the Kolmogorov "one-third" law.

Let us calculate the typical width of a spectral line formed in a turbulent medium obeying the one-third law. A somewhat more rigorous treatment of the Kolmogorov-Obukhov model yields the approximate velocity autocorrelation function (e.g., Panchev 1971):

$$C(\tau) = 1 - \left[\frac{(\pi)^{1/2}}{2\Gamma(7/6)}\right]\left(\frac{\tau}{\lambda_o}\right)^{2/3}, \quad \lambda_i < \tau < \lambda_o . \tag{25}$$

The numerical constant in the square brackets has a value of 0.96. In Paper III we demonstrate that the velocity dispersion of an optically thin molecular line, averaged over a homogeneous plane-parallel cloud line-of-sight depth L, is related to the autocorrelation function of the velocity field by

$$\sigma_i^2 \propto 1 - (2/L)\int_0^L [1 - (z/L)]C(z)dz . \tag{III-25}$$

Substituting equation (25) and integrating then yields the average full width at half-intensity,

$$\Delta v = (8 \ln 2)^{1/2}\sigma_i \sim (\text{const})(L/\lambda_o)^{1/3} . \tag{26}$$

Thus, to the extent that velocity dispersion–size correlations for molecular clouds can be characterized by an index indistinguishable from $\frac{1}{3}$, the observational data may be deemed consistent with the presence of Kolmogorov turbulence within the sources studied. Note further that if the observed molecular cloud size–line-width relation is taken as evidence that inertial range turbulence does pervade the dense interstellar medium, the outer scale of the turbulent cascade must be *larger* than the size of the largest cloud believed to obey the one-third law. Since $\Delta v \propto L^{\beta}$ appears to hold for molecular cloud sizes up to $L \geq 60$ pc (Larson 1981), the existence of a universal turbulent cascade therefore requires a correlation length at least some tens of parsecs in magnitude.

This condition cannot be easily reconciled with the present study's failure to resolve centroid velocity correlations in the Taurus clouds. Equation (25) implies that the correlation length of velocity fluctuations in the Kolmogorov model is $\lambda_K = 0.47\lambda_o$. This high degree of correlation results from the assumption that ϵ is constant throughout the range $\lambda_i < \lambda < \lambda_o$ and is a distinctive signature of a dissipationless turbulent cascade. Figure 1*b* illustrates the centroid velocity autocorrelation function which would be determined for a cloud containing gas motions with a Kolmogorov spectrum. It demonstrates that the correlation length seen from such a cloud is $\sim\lambda_K$ and is therefore also a significant fraction of λ_o. Thus, if turbulence in the Taurus complex indeed follows a one-third law, pronounced isotropic velocity correlations should have been detected in our data; in actuality, we find only the barest hint of them (§ III*d*). One might, of course, argue that for some reason the Taurus dark clouds do not share the more general pattern of turbulence presumed to give rise to the observed velocity-size correlation for molecular clouds. However, we have already pointed out above that the size and internal velocity dispersion of the Taurus complex are in fact entirely consistent with the general correlation trends noted by Larson (1981) or by Leung, Kutner, and Mead (1982).

The failure of the Kolmogorov-Obukhov model to adequately describe the internal motions of the Taurus complex—or, for that matter, any other molecular cloud (e.g., Scalo 1984)—is not altogether surprising. Even with its highly restrictive postulates (incompressibility and neglect of self-gravity, for example), the Kolmogorov-Obukhov model cannot be derived in a self-consistent fashion from the equations of hydrodynamics. It is not without utility: for example, (subsonic) turbulent motions within the Earth's atmosphere appear to follow the one-third velocity law as predicted by the model (Mavrokoukoulakis, Ho, and Cole 1978; Tatarskii 1961). Even in this case, however, where compressibility effects are largely unimportant, velocity correlations at three or more points in the atmosphere do not match the model's predictions, necessitating the introduction of "intermittency" corrections to the theory (cf. Frisch Sulem and Nelkin 1978; Ferrini, Marchesoni, and Vulpiani 1982). Further, the model's conceptual foundation—a one-way cascade of energy to smaller scales—ignores the fundamentally three-dimensional character of turbulence (e.g., Kraichnan and Montgomery 1980), as well as the likelihood that energy injection in the interstellar medium occurs on multiple length scales (Fleck 1985). The applicability of the Kolmogorov-Obukhov theory to the supersonic and highly compressible interstellar medium must therefore be considered *a priori* suspect (Dickman 1985).

It is occasionally suggested that the operation of the virial theorem may underlie the widespread velocity-size correlations seen in molecular clouds. In our view this is a somewhat misleading issue. Neglecting geometrical factors of order unity and the influence of magnetic fields, virial balance does require that the total velocity width of spectral line emission from a molecular cloud be related to the object's mass by $\Delta v^2 \sim GM/L \sim G\rho L^2$, where M and ρ are the cloud mass and mean density. However, this will be true irrespective of the nature of the gas motions which cause the spectral broadening (it holds true, for example, in a radially collapsing, as well as in a static, cloud [e.g., Penzias 1975]). Thus, a strong correlation between

molecular cloud size and velocity dispersion can be "explained" by the virial theorem only if by an explanation one means postulating a widespread, essentially scale-free mechanism governing the relationship between cloud size and *density*. One is left with a second global correlation to explain, one which is arguably no less fundamental than the original.

We are unable to propose a plausible origin for the line-width–size correlations which have been discussed above. Regardless of their physical origin, however, it should be emphasized that the general utility of line-width–cloud size variations as a probe of turbulence in the interstellar medium ultimately rests upon the premise that gas motions within *all* molecular clouds are part of a *single*, homogeneous velocity field which uniformly pervades the Galaxy. This assumption appears very difficult to justify given the diversity of physical conditions exhibited by molecular clouds, and in view of the fact that in the picture above such clouds must themselves be considered as density enhancements in a more global medium to which molecular observations are completely insensitive. As a consequence, we strongly advocate the use of the correlation techniques discussed in §§ II and III as more complete and less ambiguous investigative tools for the study of turbulence in interstellar clouds.

V. SUMMARY AND CONCLUSIONS

The presence of turbulence within molecular clouds may have profound consequences for the structure and evolution of these objects. The dynamical effects of a fluctuating velocity field within an interstellar cloud are determined largely by the degree of correlation possessed by the gas motions. This aspect of turbulence is described by the *autocorrelation function* (ACF) of the velocity fluctuations,

$$C(\tau) = \frac{\langle v(r)v(r+\tau)\rangle_r}{\langle v(r)v(r)\rangle_r} .$$

We have demonstrated that if an optically thin spectral line is used to map an interstellar cloud, the ACF of the positional centroid velocity fluctuations exhibited by the spectra will reproduce reasonably well the actual velocity ACF describing turbulence within the cloud (§ II). This is possible because the centroid velocity ACF at an observed lag τ' is a weighted average of the true velocity ACF, taken over all lags τ between pairs of points on each of two lines of sight through the cloud separated by τ', and the weighting function of this average emphasizes values of τ near τ'. Models indicate that for clouds many correlation lengths deep, the correlation length determined from a centroid velocity ACF will be somewhat larger than the true value. Even in the worst-case models, however, the discrepancy did not exceed a factor of 2, and in all cases the centroid ACF preserved the basic shape of the true, underlying model velocity correlation function (§ II).

Correlation techniques were applied to some 1200 ^{13}CO spectra taken at 15′ spacing (0.6 pc at $D = 140$ pc) across the Taurus dark cloud complex. The centroid velocity ACF suggests the presence of a systematic shear across the interior of the complex. This motion can be identified in the raw data as a progression of centroid velocities along the core of the complex, corresponding in magnitude to a gradient of $\Delta v/\Delta x \sim 0.25$ km s^{-1} pc^{-1}. This may represent rotation of the core or simply may be a chance anisotropy of gas motions on the largest scales sampled by the observations (§ III*c*). In either case, we conclude that the Taurus complex appears to be in virial equilibrium (§ IV*a*).

Apart from this large-scale, systematic motion, the velocity field revealed by our analysis appears to be essentially isotropic, and shows no significant degree of correlation on smaller scales (§ III*d*). The sample spacing of 0.6 pc therefore becomes an upper limit to the apparent correlation length of turbulent motions within the Taurus complex.

We have discussed this result critically in the context of recent suggestions that widely observed correlations between molecular cloud line widths and sizes may stem from the presence of a "cascade" of turbulent motions in the dense interstellar medium (§ IV*b*). We note that a model of this type necessarily entails a high degree of correlation for gas motions within *individual* molecular clouds, correlations which should be easily exposed by the centroid velocity techniques developed in the present paper. While the size and internal velocity dispersion which we determine for the Taurus system are in fact consistent with several previously determined size–line-width correlations for molecular clouds, our failure to resolve velocity correlations on scales larger than our 15′ sample spacing indicates that a cascade model of turbulence is inapplicable to the Taurus dark cloud complex. The assumptions which underlie the cascade model may themselves need reconsideration.

We are grateful to Dr. Robert C. Fleck, Jr., for his careful reading of the manuscript and for several valuable suggestions. This work was supported by NSF grant AST 82-12252 to the Five College Radio Astronomy Observatory. This is Contribution No. 586 of the FCRAO.

REFERENCES

Arny, T. 1971, *Ap. J.*, **169**, 289.
Baker, P. L. 1973, *Astr. Ap.*, **23**, 81.
Barnard, E. E. 1927, *Atlas of Selected Regions of the Milky Way*, ed. E. B. Frost and M. Calvert (*Carnegie Inst. Washington Pub.*, No. 247).
Bash, F., Hausman, M., and Papaloizou, J. 1981, *Ap. J.*, **245**, 92.
Boland, W., and de Jong, T. 1982, *Ap. J.*, **261**, 110.
Brenner, N. M. 1976, in *Methods of Experimental Physics*, Vol. **12**, Part C, ed. M. L. Meeks (New York: Academic), p. 284.
Chandrasekhar, S. 1951, *Proc. Roy. Soc. London, A*, **210**, 26.
Chièze, J. P., and Lazareff, B. 1980, *Astr. Ap.*, **91**, 290.
Dickman, R. L. 1978, *Ap. J. Suppl.*, **37**, 407.
———. 1985, in *Protostars and Planets II*, ed. D. C. Black and M. S. Matthews (Tucson: University of Arizona Press), in press.
Dickman, R. L., and Kleiner, S. C. 1985, *Ap. J.*, **295**, 479 (Paper III).
Eckmann, J. P. 1981, *Rev. Mod. Phys.*, **53**, 643.
Elias, J. 1978, *Ap. J.*, **224**, 857.
Ferrini, F., Marchesoni, F., and Vulpiani, A. 1982, *Phys. Letters, A*, **92**, 47.
Fleck, R. C. 1980, *Ap. J.*, **242**, 1019.
———. 1985, *Ap. J. (Letters)*, in press.
Franco, J. 1983, *Ap. J.*, **264**, 508.
Friedlander, S. K., and Topper, L. (eds.) 1961, *Classic Papers on Statistical Theory of Turbulence* (New: York: Interscience).
Frisch, U., Sulem, P. U., and Nelkin, M. 1978, *J. Fluid Mech.*, **97**, 719.
Hunter, J. H., and Fleck, R. C., Jr. 1982, *Ap. J.*, **256**, 505.
Kampé de Fériet, J. 1955, in *Gas Dynamics of Cosmic Clouds* (Amsterdam: North-Holland), p. 134.
Kaplan, S. A., and Klimishin, I. A. 1964, *Soviet Astr.—AJ*, **8**, 210.
Kleiner, S. C., and Dickman, R. L. 1984, *Ap. J.*, **286**, 255 (Paper I).
———. 1985, in preparation.
Kraichnan, R. H., and Montgomery, D. 1980, *Rept. Progr. Phys.*, **43**, 537.
Landau, L. D., and Lifshitz, E. M. 1959, *Fluid Mechanics* (London: Pergamon).

Larson, R. 1979, *M.N.R.A.S.*, **186**, 479.
———. 1981, *M.N.R.A.S.*, **194**, 809.
Leslie, D. C. 1973, *Developments in the Theory of Turbulence* (Oxford: Clarendon).
Leung, C. M., Kutner, M. L., and Mead, K. M. 1982, *Ap. J.*, **262**, 583.
Lumley, J. 1971, in *Statistical Models and Turbulence*, ed. M. Rosenblatt and C. Van Atta (Berlin: Springer).
Lynds, B. T. 1962, *Ap. J. Suppl.*, **7**, 1.
Mavrokoukoulakis, N. D., Ho, K. L., and Cole, R. S. 1978, *IEEE Trans. Antenna Prop.*, **AP26**, 875.
Münch, G. 1958, *Rev. Mod. Phys.*, **30**, 1035.
Myers, P. C. 1983, *Ap. J.*, **270**, 105.
Panchev, S. 1971, *Random Functions and Turbulence* (Oxford: Pergamon).
Penzias, A. A. 1975, in *Les Houches XXVI, Atomic and Molecular Physics and Interstellar Matter*, ed. R. Balian, P. Encrenaz, and J. Lequeux (Amsterdam: North-Holland), p. 373.
Regev, O., and Shaviv, G. 1981, *Ap. J.*, **245**, 934.
Roczyczka, M., Tscharnuter, W. M., and Yorke, H. W. 1980, *Astr. Ap.*, **81**, 347.
Sasao, T. 1971, *Pub. Astr. Soc. Japan*, **23**, 433.
Scalo, J. M. 1984, *Ap. J.*, **277**, 556.
Scalo, J. M., and Pumphrey, W. A. 1982, *Ap. J. (Letters)*, **258**, L29.
Tatarskii, V. I. 1961, *Wave Propagation in a Turbulent Medium* (New York: McGraw-Hill).
Tennekes, H., and Lumley, J. L. 1972, *A First Course in Turbulence* (Cambridge: MIT Press).

ROBERT L. DICKMAN and STEVEN C. KLEINER: Radio Astronomy, Graduate Research Center, University of Massachusetts, Amherst, MA 01003

THE ASTROPHYSICAL JOURNAL, 295: 479–484, 1985 August 15

LARGE-SCALE STRUCTURE OF THE TAURUS MOLECULAR COMPLEX. III. METHODS FOR TURBULENCE

R. L. DICKMAN AND S. C. KLEINER
Five College Radio Astronomy Observatory; and Department of Physics and Astronomy, University of Massachusetts
Received 1984 October 18; accepted 1985 February 25

ABSTRACT

This paper presents a unified exposition of methods which permit the quantitative study of turbulent motions within interstellar clouds; it is a companion to the accompanying work on the velocity field of the Taurus molecular cloud complex. The basic method discussed here—which is at least some 30 years old—involves mapping a source in an optically thin spectral line, and studying the spatial correlation properties of the resulting velocity centroid map.

We first establish the relationship between the centroid of an optically thin spectral transition and the average velocity of gas along the line formation path. We then show how the correlation length and amplitude of turbulence in a source are reflected in the statistical behavior of spectral line centroids. Some useful general relations, which basically stem from simple dimensional arguments, are noted in this context. Finally, we also consider the impact of data noise on derived velocity field parameters, and describe methods for assessing its magnitude and correcting for its influence.

Subject headings: interstellar: molecules — turbulence

I. INTRODUCTION

This paper presents a unified exposition of methods which permit the quantitative study of turbulent motions within interstellar clouds. It forms a companion to our study of the large-scale velocity structure of the Taurus dark cloud complex (Kleiner and Dickman 1985*a*, hereafter Paper II) and to our subsequent work on turbulence in Heiles's Cloud 2 (Kleiner 1985; Kleiner and Dickman 1985*b*, hereafter Paper IV).

The notion that mapping spectral lines in a turbulent medium can provide quantitative information concerning the correlation structure of the turbulence is at least 30 years old (Kampé de Fériet 1955). The period since has seen occasional application of these ideas to the interstellar medium by, for example, Münch (1958), Kaplan and Klimishin (1964), Baker (1976), and Chièze and Lazareff (1980), among others. However, to our knowledge there has been no unified presentation of the concepts which underlie these studies. This is unfortunate for a number of reasons. While the theoretical principles involved in the present work are straightforward, the simplifications necessary to yield a tractable analysis scheme are not minor; critical scrutiny of the assumptions made in doing so will be necessary for future refinements of method. Second, for reasons discussed in detail elsewhere (Kleiner and Dickman 1984, 1985*b*; Dickman 1985; Kleiner 1985), our work utilizes autocorrelation, rather than structural, measures to characterize observational data; this is in sharp contrast to the studies cited above. Finally, our primary concern is to place the study of turbulence in molecular clouds firmly in the *observational* arena. Thus, in addition to the inevitable theoretical accommodations noted above, one must also be prepared to deal with the complications introduced by noisy data. To our knowledge, this has not yet been done.

The analysis presented here is by no means exhaustive, and a basic familiarity with correlation measures and their physical relevance to the interstellar medium is presumed on the part of the reader (see references in Kleiner 1985; Kleiner and Dickman 1984, 1985*a*; Scalo 1984; reviews by Scalo 1985 and Dickman 1985). The paper is organized into two sections. The first establishes the relationship between the velocity centroid of an optically thin spectral line in a homogeneous source and the underlying velocity field. It then shows how the correlation length and amplitude of turbulence in the source are reflected in the statistical behavior of the spectral centroids; some useful general relationships which follow from dimensional arguments are pointed out. The concluding section of the paper considers the degradation produced by instrumental noise in estimates of velocity autocorrelation functions, and describes methods for gauging its magnitude and correcting for its influence.

II. ANALYSIS OF VELOCITY FLUCTUATIONS

a) *Magnitude of Velocity Fluctuations*

Let $v(x, y, z)$ denote the line-of-sight velocity component of gas motions at a position (x, y, z) within a homogeneous, plane-parallel cloud of depth L. Define the vectors $\boldsymbol{r}$ and $\boldsymbol{r}'$ as

$$\boldsymbol{r} = x\hat{\boldsymbol{x}} + y\hat{\boldsymbol{y}} + z\hat{\boldsymbol{z}} , \tag{1a}$$

$$\boldsymbol{r}' = x'\hat{\boldsymbol{x}} + y'\hat{\boldsymbol{y}} + z'\hat{\boldsymbol{z}} , \tag{1b}$$

where the unit vectors are taken such that the $\hat{\boldsymbol{x}}$-$\hat{\boldsymbol{y}}$ plane coincides with the face of the cloud, and $\hat{\boldsymbol{z}}$ lies along the line of sight away from the observer. We shall express the specific intensity of a spectral line above the adjacent continuum at frequency ν as an antenna temperature at velocity offset u; hence, if ν_0 is the rest frequency of the transition, then u is the velocity corresponding to a Doppler shift $(\nu_0 - \nu)$:

$$u \equiv \left(\frac{\nu_0 - \nu}{\nu_0}\right)c - u_0 . \tag{2}$$

The constant u_0 defines the origin of the observer's velocity scale.

In what follows we shall ignore background sources of radiation, and shall work in the Rayleigh-Jeans approximation;

this entails no loss of generality. Letting $T_a(u; x, y)$ denote the normally emergent emission at velocity u from position (x, y) on the face of the model cloud, and letting $T_x(\boldsymbol{r})$ denote the excitation temperature of the emitting gas at $\boldsymbol{r}$, the solution of the equation of radiative transfer may then be written

$$T_a(u; x, y) = \int_0^{t(u;x,y,L)} T_x(\boldsymbol{r})\, e^{-t(u;\boldsymbol{r})} dt(u; \boldsymbol{r}) . \quad (3)$$

The quantity $t(u; \boldsymbol{r}) \equiv t(u; x, y, z)$ is the optical depth at Doppler velocity u and position (x, y), measured from the rear of the cloud to z. It is related to the absorption coefficient of the gas by

$$t(u; \boldsymbol{r}) \equiv \int_0^z \kappa_0(\boldsymbol{r}')\phi[u; v(\boldsymbol{r}')]dz' . \quad (4)$$

Here $\kappa_0(\boldsymbol{r})$ is the integrated absorption coefficient, which depends only upon the excitation conditions of the emitting gas at $\boldsymbol{r}$, and $\phi[u; v(\boldsymbol{r})]$ is the local line profile function, which is a function of u (the velocity equivalent of the radiation frequency in the observer's rest frame) and $v(\boldsymbol{r})$, the line-of-sight gas velocity at $\boldsymbol{r}$.

The line-profile function obeys the normalization

$$\int \phi[u; v(\boldsymbol{r})]du \equiv 1 , \quad (5)$$

where the integration is performed over the spectral line in question. This integration is usually defined in the frequency domain over the range $(0, \infty)$, but upon transforming to the velocity variable u, and utilizing the fact that ϕ is a strongly peaked function, it is permissible to extend the integration over u to the range $(-\infty, \infty)$. We shall assume that $\phi[u; v(\boldsymbol{r})]$ is symmetric about $u = 0$ in the rest frame of the gas at $\boldsymbol{r}$, and that the Doppler shift is the only process which couples the inferred velocity u with the line-of-sight component of the gas motions. In that case,

$$\phi[u; v(\boldsymbol{r})] = \phi[u - v(\boldsymbol{r})] . \quad (6)$$

For optically thin emission, $t(u; x, y, L) \ll 1$, and equation (3) becomes simply

$$T_a(u; x, y) = \int_0^L T_x(\boldsymbol{r})\kappa_0(\boldsymbol{r})\phi[u - v(\boldsymbol{r})]dz . \quad (7)$$

The centroid velocity of the molecular line profile observed at position (x, y) on the cloud face is defined as

$$v_c(x, y) = \frac{\int T_a(u; x, y)udu}{\int T_a(u; x, y)du} . \quad (8)$$

Again, the integrations are carried out over the spectral profile, and can be extended to the range $(-\infty, \infty)$. From equation (7), the denominator of this expression is

$$\int_{-\infty}^{\infty} T_a(u; x, y)du = \int_0^L T_x(\boldsymbol{r})\kappa_0(\boldsymbol{r})dz \int_{-\infty}^{\infty} \phi[u - v(\boldsymbol{r})]du . \quad (9)$$

Changing the velocity variable to $q \equiv u - v(\boldsymbol{r})$, and using the normalization in equation (5), result in

$$\int_{-\infty}^{\infty} T_a(u; x, y)du = \int_0^L T_x(\boldsymbol{r})\kappa_0(\boldsymbol{r})dz \int_{-\infty}^{\infty} \phi(q)dq = \int_0^L T_x(\boldsymbol{r})\kappa_0(\boldsymbol{r})dz . \quad (10)$$

Similarly, the numerator of equation (8) may be written as

$$\int_{-\infty}^{\infty} T_a(u; x, y)udu = \int_0^L T_x(\boldsymbol{r})\kappa_0(\boldsymbol{r})dz \int_{-\infty}^{\infty} [q + v(\boldsymbol{r})]\phi(q)dq . \quad (11)$$

The inner integral can be expanded:

$$\int_{-\infty}^{\infty} [q + v(\boldsymbol{r})]\phi(q)dq = v(\boldsymbol{r}) \int_{-\infty}^{\infty} \phi(q)dq + \int_{-\infty}^{\infty} q\phi(q)dq . \quad (12)$$

By reference to equation (5), the first term on the right-hand side is seen to be simply $v(\boldsymbol{r})$, and the second vanishes because of the symmetry of $\phi(q)$. Thus, the velocity centroid of an optically thin spectral line is

$$v_c(x, y) = \frac{\int_0^L v(\boldsymbol{r})T_x(\boldsymbol{r})\kappa_0(\boldsymbol{r})dz}{\int_0^L T_x(\boldsymbol{r})\kappa_0(\boldsymbol{r})dz} . \quad (13)$$

Within a homogeneous cloud, $\kappa_0(\boldsymbol{r})$ and $T_x(\boldsymbol{r})$ are constant, and $v_c(x, y)$ therefore becomes the mean gas velocity along the line of sight through (x, y):

$$v_c(x, y) = (1/L)\int_0^L v(\boldsymbol{r})dz \equiv \langle v(\boldsymbol{r})\rangle_z , \quad (14)$$

where angle brackets denote an average over the subscripted variable.

Homogeneity is obviously an unrealistic assumption to apply to all but the most diffuse and undifferentiated interstellar clouds. However, the product $T_x\kappa_0$ appears in both the numerator and the denominator of equation (13). Hence, to lowest order, departures from homogeneity will leave equation (14), and the results which follow hereafter, essentially unchanged.

The mean value of $v_c(x, y)$ is also the mean velocity of gas within the molecular cloud:

$$\langle v_c(x, y)\rangle_{x,y} = \langle\langle v(\boldsymbol{r})\rangle_z\rangle_{x,y} = \langle v(\boldsymbol{r})\rangle_{x,y,z} \equiv \langle v\rangle . \quad (15)$$

We shall assume through the remainder of this work that the origin of the velocity scale in equation (2) has been chosen so that $u = 0$ corresponds to $\langle v\rangle$. This will simplify the notation somewhat in the manipulations which follow.

b) *Velocity Dispersions*

Three statistical measures which characterize the gas motions within a molecular cloud may now be introduced. These are the *parent*, *internal*, and *centroid* velocity dispersions, σ_p, σ_i, and σ_c, respectively. With the simplifying assumption that $\langle v\rangle = 0$, these are defined by the relations

$$\sigma_p^2 \equiv \langle v^2(\boldsymbol{r})\rangle_{\boldsymbol{r}} , \quad (16)$$

$$\sigma_i^2 \equiv \langle\langle[v(\boldsymbol{r}) - \langle v(\boldsymbol{r})\rangle_z]^2\rangle_z\rangle_{x,y} , \quad (17)$$

$$\sigma_c^2 \equiv \langle[\langle v(\boldsymbol{r})\rangle_z]^2\rangle_{x,y} . \quad (18)$$

The parent dispersion measures the total magnitude of velocity fluctuations within a molecular cloud. It is most easily estimated from a set of observations by forming the collective spectral profile of the data (see Paper II, for example). By contrast, the internal dispersion characterizes the rms magnitude of gas motions along individual lines of sight with respect to the average velocities along those directions; σ_i is thus essentially a characteristic width for the individual spectra which comprise the data set. The last quantity, σ_c^2, is simply the ensemble variance of these line-of-sight average velocities. The

three measures are not independent; from equations (17) and (18),

$$\sigma_p^2 = \sigma_i^2 + \sigma_c^2 . \tag{19}$$

The quantities σ_i^2 and σ_c^2 can both be derived from a set of spectral line observations. The velocity dispersion of a line profile at (x, y) is

$$\sigma_i^2(x, y) = \frac{\int T_a(u; x, y)[u - v_c(x, y)]^2 du}{\int T_a(u; x, y) du} . \tag{20}$$

Substituting the solution (7) of the optically thin, homogeneous transport equation into equation (20) then leads directly to equation (17), provided that one makes the obvious identification

$$\sigma_i^2 = \langle \sigma_i^2(x, y) \rangle_{x,y} . \tag{21a}$$

Trivial application of equations (14) and (15) yields

$$\sigma_c^2 = \langle (v_c^2(x, y) \rangle_{x,y} . \tag{21b}$$

Thus σ_c^2 can be calculated directly from a set of observational data. However, it can also be expressed theoretically in terms of the two-point autocorrelation function of the source velocity field, provided that the latter is assumed to be isotropic. *This therefore provides a direct link between the spectral line map of an interstellar cloud and the simplest statistical measure of turbulence within the object.* In order to derive this relationship, one substitutes the definition of $v_c(x, y)$ given by equation (14) into equation (21b):

$$\langle v_c^2(x, y) \rangle_{x,y} \equiv \langle v_c^2 \rangle = (1/L^2) \left\langle \int v(\mathbf{r}) dz \int v(\mathbf{r}') dz' \right\rangle_{x,y} . \tag{22}$$

Since the average is performed over x and y coordinates, while the integration is carried out over z, the integration and averaging operations may be interchanged. Thus,

$$\langle v_c^2 \rangle = (1/L^2) \iint \langle v(\mathbf{r}) v(\mathbf{r}') \rangle_{x,y} dz dz' . \tag{23}$$

The integrand, however, is simply $\sigma_p^2 C(|z - z'|)$, where C is the longitudinal autocorrelation function of the velocity field (see Paper II). Because C is even under an exchange of z and z', a simple change of variable (e.g., Chandrasekhar and Münch 1952; Tatarskii 1961) allows equation (23) to be expressed as

$$\sigma_c^2 = (2\sigma_p^2/L) \int [1 - (z/L)] C(z) dz . \tag{24}$$

Since σ_p^2 can be estimated from the same observational data which yield the value of σ_c (cf. above and Paper II), equation (24) provides a basic link between the longitudinal ACF of the source velocity field and two simple statistical measures which characterize the spectral line map of the cloud. An alternative form of this relation is provided by using equation (19):

$$\sigma_i^2 = \sigma_p^2 [\![1 - \{(2/L) \int_0^L [1 - (z/L)] C(z) dz \}]\!] . \tag{25}$$

If the depth of an interstellar cloud appreciably exceeds its largest turbulent correlation scale—which we will denote λ_c—one can make a rough estimate of the latter quantity from a set of observations without explicit recourse to the velocity correlation function. Consider a set of N *independent* observations of a random variable v. Very simple statistical arguments demonstrate that the variance of the mean value of v averaged over N observations is related to the variance of v itself by

$$\langle \langle v \rangle^2 \rangle = \langle v^2 \rangle / N . \tag{26}$$

If v is considered to be the line-of-sight velocity field, the number of *independent* samples along a particular sight line is roughly the number of correlation lengths there, $N \sim (L/\lambda_c)$. Thus, $\sigma_c^2 \sim \sigma_p^2(\lambda_c/L)$. Defining $h = (\sigma_i^2/\sigma_c^2)$, equation (19) indicates that $(\lambda_c/L) \sim (1/h + 1)$. If one estimates the cloud depth L by any of several strategies, one can therefore obtain λ_c from the ratio of dispersions given above. It may be worthwhile to emphasize that λ_c is defined above by the criterion that it correspond to the distance over which the velocity field decorrelates completely. As a result, λ_c is likely to be several times larger than the more conventionally used turbulent correlation length (the scale over which correlations relax to a level e^{-1} their maximum value).

c) *ACF of Centroid Velocity Fluctuations*

In this section we examine the relationship between the autocorrelation function (ACF) of spectral line centroid velocity fluctuations and the velocity ACF which characterizes the turbulent medium. For simplicity we assume that any systematic motions discernible in the data have been removed by filtering or by other suitable methods (see Paper II; Kleiner 1985), and that the remaining motions are isotropic. The velocity covariance and correlation functions therefore depend only on $|\tau'|$, and since $c'(-\tau') = c'(\tau')$, we shall denote the argument of these functions simply as τ'. The autocovariance function of the centroid velocity fluctuations is defined as

$$c'(\tau') = \langle v_c(x, y) v_c(x', y') \rangle_{x,y} . \tag{27}$$

Here (x, y) and (x', y') denote pairs of points separated by τ',

$$\tau'^2 = (x - x')^2 + (y - y')^2 , \tag{28}$$

and it is assumed that the velocity scale of the observations has been adjusted so that $\langle v_c(x, y) \rangle_{x,y} = \langle v \rangle = 0$.

The corresponding autocorrelation function is given by

$$C'(\tau') = c'(\tau')/c'(0) . \tag{29}$$

We note that $c'(0)$ is simply the variance of the centroid velocity fluctuations:

$$c'(0) \equiv \langle v_c^2(x, y) \rangle_{x,y} \equiv \sigma_c^2 . \tag{30}$$

For optically thin emission lines (cf. eq. [14]),

$$v_c(x, y) = (1/L) \int_0^L v(\mathbf{r}) dz ,$$

so that

$$c'(\tau') = \left\langle (1/L^2) \int v(x, y, z) dz \int v(x', y', z') dz' \right\rangle_{x,y} . \tag{31}$$

Inverting the order in which the integration and the average are performed,

$$c'(\tau') = (1/L^2) \iint \langle v(x, y, z) v(x', y', z') \rangle_{x,y} dz dz' . \tag{32}$$

The integrand is the longitudinal autocovariance of the gas motions within the cloud; referring to equation (28), it may be written $c\{[\tau'^2 + (z - z')^2]^{1/2}\}$. As in the derivation of equation (24), the symmetry of $C(\tau)$ under inversion may be exploited to

simplify the double integral. Using equation (29),

$$C'(\tau') = \frac{\int_0^L [1 - (z/L)] C[(\tau'^2 + z^2)^{1/2}] dz}{\int_0^L [1 - (z/L)] C(z) dz} . \quad (33)$$

The observed correlation function at lag τ' is therefore a triangle-weighted average of $C(\tau)$, formed with τ running over all possible spacings between points on each of two sight lines spaced by τ'. This weighting tends to emphasize values of $C(\tau)$ for which $\tau \sim \tau'$, and since $C(\tau)$ is generally a decreasing function of τ (Lumley 1970), one thus expects $C'(\tau')$ to be a reliable estimator of the true velocity ACF. This is illustrated explicitly in Paper II, where equation (33) is evaluated for several different forms of $C(\tau)$.

III. EFFECT OF INSTRUMENTAL NOISE

a) *Degradation of the ACF*

Instrumental noise induces spurious variations in the calculated centroid velocities of molecular line profiles. These fluctuations are spatially random and reduce the apparent magnitude of any correlations present in the data. To explore how this occurs and how it may be compensated for, let us denote by $v_c(x, y)$ and $v_c^*(x, y)$ centroid velocities observed at (x, y) in the presence and absence of radiometer noise, respectively. If the noise-induced error in determining the centroid velocity is denoted by $\delta v_c(x, y)$, then clearly

$$v_c(x, y) = v_c^*(x, y) + \delta v_c(x, y) . \quad (34)$$

One expects the velocity fluctuations induced by instrumental noise to be spatially uncorrelated with zero mean. Denoting their variance by σ_n^2, we then have

$$\langle \delta v_c(x, y) \rangle_{x,y} = 0 , \quad (35a)$$

for

$$\langle \delta v_c(x, y) \delta v_c(x', y') \rangle_{x,y} = \sigma_n^2 \quad [(x - x')^2 + (y - y')^2 = 0]$$
$$= 0 \quad [(x - x')^2 + (y - y')^2 \neq 0] . \quad (35b)$$

The autocovariance of the centroid velocity fluctuations is defined (eq. [27] above; Paper II):

$$c'(\boldsymbol{\tau}') = \langle v_c(x, y) v_c(x', y') \rangle_{x,y} , \quad (36a)$$

where

$$\tau'^2 = (x - x')^2 + (y - y')^2 . \quad (36b)$$

Substituting equation (34) yields

$$c'(\boldsymbol{\tau}') = \langle [v_c(x, y) + \delta v_c(x, y)][v_c(x', y') + \delta v_c(x', y')] \rangle_{x,y} . \quad (36c)$$

Using equations (36a) and (36c), we thus find that at nonzero lags the value of the autocovariance function remains unchanged by the noise, i.e.,

$$c'(\boldsymbol{\tau}') = c^*(\boldsymbol{\tau}'), \quad \boldsymbol{\tau}' \neq 0 , \quad (37a)$$

where we have used $c^*(\boldsymbol{\tau}')$ to denote the noise-free centroid velocity autocovariance function. At zero lag, however,

$$c'(0) = c^*(0) + \sigma_n^2 = \sigma_c^{*2} + \sigma_n^2 , \quad (37b)$$

where σ_c^{*2} is the noise-free variance of centroid velocity fluctuations. The observed autocorrelation function is

$$C'(\boldsymbol{\tau}) \equiv c'(\boldsymbol{\tau})/c'(0) . \quad (38)$$

Equations (37a) and (37b) thus imply a *reduction* in the apparent magnitude of correlations at nonzero lags given by

$$\frac{C'(\boldsymbol{\tau}')}{C^*(\boldsymbol{\tau}')} = \left[1 + \left(\frac{\sigma_n}{\sigma_c^*}\right)^2\right]^{-1}, \quad \boldsymbol{\tau}' \neq 0 , \quad (39)$$

where $C^*(\boldsymbol{\tau}')$ is the noise-free centroid velocity ACF.

The quantity σ_c^{*2} cannot be measured directly. However, $v_c(x, y)$ and $\delta v_c(x, y)$ are mutually independent variables; hence we may put

$$\sigma_c^{*2} = \sigma_c^2 - \sigma_n^2 . \quad (40)$$

Substituting equation (40) in equation (39) and rearranging finally yield

$$\frac{C'(\boldsymbol{\tau}')}{C^*(\boldsymbol{\tau}')} = 1 - \left(\frac{\sigma_n}{\sigma_c}\right)^2, \quad \boldsymbol{\tau}' \neq 0 . \quad (41)$$

By simple rescaling, equation (41) enables one to correct an autocorrelation function calculated from noisy data. However, in order to do so, one must estimate the impact which radiometer fluctuations have upon the velocity centroid estimation process, i.e., one must determine σ_n. We consider this point next.

b) *Estimation of* σ_n

In spectral line observations, radiometer noise is usually characterized by the variance of the antenna temperature fluctuations which occur in each spectrometer channel. The mean error associated with measuring the velocity centroid of a noisy line must depend upon the amplitude of these fluctuations, as well as upon a number of additional factors. These include the intensity and width of the line itself, the resolution of the spectrometer, as well as the way in which the line is centered with respect to the spectrometer (important only when the emission or absorption features under study are only a few resolution elements wide). For example, the stronger a line, the less significant the effect of receiver noise. In this section we consider three independent methods for estimating the rms uncertainty of velocity centroids in a noisy data set.

In principle, σ_n may be calculated directly from the probability density function of δv_c. To determine this function, we first decompose the antenna temperature measured in a filter-bank channel i into the true antenna temperature due to emission from the cloud, and a noise component. [Since the following discussion deals with a single spectral line, specifying coordinates (x, y) is unnecessary and is omitted for clarity.] Retaining the convention that starred quantities are those which would be observed in the absence of noise, we write this as

$$T_i(x, y) = T_i^*(x, y) + \delta T_i(x, y) . \quad (42)$$

The temperature fluctuations δT_i are assumed to have a Gaussian distribution, with zero mean, dispersion δT_a, and to be uncorrelated across different spectrometer channels:

$$\langle \delta T_i \rangle = 0 \quad (43a)$$

and

$$\langle \delta T_i \delta T_j \rangle = 0 \quad \text{if } i \neq j$$
$$= \delta T_a^2 \quad \text{if } i = j . \quad (43b)$$

The centroid velocity of a spectral line observed in the presence of instrumental noise is

$$v_c = \frac{\sum_{i=1}^N T_i u_i}{\sum_1^N T_i} = \frac{\sum_1^N T_i^* u_i + \sum_1^N \delta T_i u_i}{\sum_1^N T_i^* + \sum_1^N \delta T_i} , \quad (44)$$

where u_i is the velocity assigned to the center of spectrometer channel i. The summation in this and following equations ranges over channels 1 through N. This defines the velocity range (or *window*) over which centroids are calculated. In order to simplify the following work, we shall assume that the chosen velocity window is centered upon, and symmetric about, v_c^*, the noise-free centroid velocity:

$$v_c^* = \frac{\sum T_i^* u_i}{\sum T_i^*} = 0 \tag{45}$$

and

$$\sum u_i = 0 \, . \tag{46}$$

Under these conditions, the noise-induced error in a centroid velocity determination becomes

$$\delta v_c = \frac{\sum \delta T_i u_i}{\sum T_i^* + \sum \delta T_i} \, . \tag{47}$$

The problem thus becomes one of calculating $\langle \delta v_c^2 \rangle \equiv \sigma_n^2$. We note that the sum of Gaussian random variables, as well as the product and sum of a constant and a Gaussian random variable, all retain Gaussian distributions. Hence, the centroid fluctuations induced by noise are a quotient of two Gaussian random variables. With the specific choice of velocity scale given by equation (45), these variables are uncorrelated and therefore independent:

$$\langle \sum \delta T_i u_i \sum \delta T_j \rangle = \sum_i \sum_j u_i \langle \delta T_i \delta T_j \rangle = \delta T_a^2 \sum_i u_i = 0 \, . \tag{48}$$

Now $f_Z(Z)$, the probability density of a random variable $Z = X/Y$, where X and Y are themselves random variables, can be written (Papoulis 1965)

$$f_Z(Z) = \int_0^\infty Y f_{XY}(ZY, Y) dY - \int_{-\infty}^0 Y f_{XY}(ZY, Y) dY \, , \tag{49}$$

where $f_{XY}(X, Y)$ is the probability of finding a joint occurrence of X and Y. If X and Y are independent and Gaussian, their joint density is simply (Papoulis 1965)

$$f_{XY}(X, Y) = (2\pi\sigma_X \sigma_Y)^{-1} \times \exp\left[-\frac{(X - \langle X \rangle)^2}{2\sigma_X^2} - \frac{(Y - \langle Y \rangle)^2}{2\sigma_Y^2} \right] , \tag{50}$$

where σ_X, $\langle X \rangle$, and σ_Y, $\langle Y \rangle$ are the standard deviations and means of X and Y, respectively. If we put (cf. eq. [47])

$$X = \sum \delta T_i u_i \, , \tag{51}$$

$$Y = \sum T_i^* + \sum \delta T_i \, , \tag{52}$$

$$\delta v_c = Z = X/Y \, , \tag{53}$$

the first and second moments of X and Y can be calculated with the aid of equations (43a) and (43b):

$$\langle X \rangle = 0 \, , \tag{54}$$

$$\sigma_X^2 = \langle X^2 \rangle - \langle X \rangle^2 = \delta T^2 \sum u_i^2 \, , \tag{55}$$

$$\langle Y \rangle = \sum T_i^* \, , \tag{56}$$

$$\sigma_Y^2 = \langle Y^2 \rangle - \langle Y \rangle^2 = \delta T^2 \, . \tag{57}$$

We note that the size of the velocity window enters the calculation of σ_n only through equation (55).

Once the density $f_Z(Z)$ is calculated from equation (49), the magnitude of the noise-induced fluctuations in the calculated centroid velocities is

$$\sigma_n^2 = \sigma_Z^2 = \int_{-\infty}^{\infty} Z^2 f_Z(Z) dZ \, . \tag{58}$$

Although equations (49–(58) provide the basis for an exact determination of σ_n^2, their evaluation rapidly becomes exceedingly cumbersome. A more serviceable and physically transparent approach to the calculation of noise effects is achieved by considering the estimation of σ_n^2 as a problem in the propagation of errors. Retaining the notation and velocity scale above, the variance of Z can be approximated in terms of the variances of X and Y (e.g., Bevington 1969):

$$\sigma_n^2 = \sigma_Z^2 \approx \frac{X_0^2}{Y_0^2} \left(\frac{\sigma_X^2}{X_0^2} + \frac{\sigma_Y^2}{Y_0^2} \right) = \frac{\sigma_X^2}{Y_0^2} + \frac{X_0^2 \sigma_Y^2}{Y_0^4} \, . \tag{59}$$

In this equation, X_0 and Y_0 are the mean values of X and Y,

$$X_0 = \langle X \rangle = \langle \sum T_i^* u_i \rangle = 0 \, , \tag{60}$$

$$Y_0 = \langle Y \rangle = \langle \sum T_i^* + \sum \delta T_i \rangle = \sum T_i \, , \tag{61}$$

and, as above,

$$\sigma_X^2 = \delta T^2 \sum_{i=1}^{N} u_i^2 \, , \tag{55}$$

where N is the number of channels within the velocity window. For N odd (as required by the assumption of a velocity window symmetric about $u = 0$) the sum in equation (55) may be rewritten as

$$\sum_{1=1}^{N} u_i^2 = 2\delta u^2 \sum_{i=1}^{M} (i - \tfrac{1}{2})^2 \, , \quad M = (N - 1)/2 \, , \tag{62}$$

where δu denotes the velocity width of a spectrometer channel. Expanding the sum and substituting in equation (59) yields

$$\sigma_n^2 = \delta T^2 \delta u^2 (4M^3 - M)/6(\sum T_i)^2 \, , \quad M = (N - 1)/2 \, . \tag{63}$$

In order to show more clearly the dependence of σ_n^2 upon typical observed line parameters, we neglect the term linear in M and take $N \approx N - 1$, so that now

$$\sum_{i=1}^{N} u_i^2 \approx \frac{\delta u^2 N^3}{12} \tag{64}$$

and

$$\sigma_n^2 \approx \frac{\delta u^2 N^3 \delta T^2}{12(\sum T_i)^2} \, . \tag{65}$$

Except for a factor δu, the sum in the denominator of equation (65) is the integrated intensity of the mean line profile. If the shape of a typical spectral profile is assumed to be Gaussian, this sum may be expressed in terms of $\Delta v_{\rm FWHM}$ and $T_{\rm peak}$, the full width at half-maximum and the peak intensity of the profile, respectively:

$$(\sum T_i)^2 \approx \left(\frac{\pi}{4 \ln 2} \right) \frac{T_{\rm peak}^2 \Delta v_{\rm FWHM}^2}{\delta u^2} \, . \tag{66}$$

Then equation (65) becomes

$$\sigma_n^2 \approx \left(\frac{\ln 2}{3\pi} \right) \left(\frac{\delta T}{T_{\rm peak}} \right)^2 \left(\frac{\delta u}{\Delta v_{\rm FWHM}} \right)^2 N^3 \delta u^2 \, . \tag{67}$$

The variance of centroid fluctuations thus depends sensitively

on the size of the velocity window used to analyze the data ($\sim N^3$). Therefore, in calculating centroid velocities from a set of observed spectra, it is advisable to choose a velocity window just large enough to include the data. An obvious choice, for example, might be a window $6\sigma_p$ wide, where σ_p^2 is the full variance of gas motions within the cloud under observation (see eqs. [15]–[17] in § II; a discussion of some practical problems in implementing this strategy is given in Paper II).

It should be borne in mind that, despite its transparency, the result above is approximate. For the analysis given in both Paper II and Paper IV, we have found it most useful to determine σ_n^2 by statistical simulations. One simply performs a numerical experiment in which a synthetic filter bank is filled with a model line profile. For each of many trials, the apparent centroid velocity is calculated before and after the addition of Gaussian noise appropriate to the data set to each filter-bank channel. The rms value of the change in centroid velocities induced by the addition of the noise is then taken as σ_n. The parameters of the Gaussian test line profile should be set by the average intensity and width of one's observed profiles. It is also important to allow the placement of the model spectral line peak to vary within the model filter bank, although, as noted above, the resultant error amplitude will depend strongly upon this placement only when one is dealing with spectra relatively narrow compared with the spectrometer channel width. For example, in dealing with the ^{13}CO spectra which form the basis of the velocity analyses given in Papers II and IV, spectra typically ~ 4 channels across at half-power, this was not found to be a significant source of uncertainty in our estimates for σ_n. As a final matter, it should be noted that because σ_n depends upon one's estimate for the noise-free width of a typical spectral line (which we have denoted σ_c^*), one must generally iterate a numerical simulation for σ_n, continually refining one's estimate for σ_c^*. Referring again to our work on ^{13}CO in the Taurus complex, it was found that a few iterations quickly produced estimates satisfying the self-consistency requirement that $\sigma_c^2 = \sigma_c^{*2} + \sigma_n^2$.

We are grateful to Dr. Robert Fleck for his careful review of this manuscript. This work was supported by National Science Foundation grant AST82-12252 to the Five College Radio Astronomy Observatory. This is Contribution No. 592 of the FCRAO.

REFERENCES

Baker, P. L. 1976, *Astr. Ap.*, **50**, 327.
Bevington, P. R. 1969, *Data Reduction and Error Analysis for the Physical Sciences* (New York: McGraw-Hill).
Chandrasekhar, S., and Münch, G. 1952, *Ap. J.*, **115**, 103.
Chièze, J. P., and Lazareff, B. 1980, *Astr. Ap.*, **91**, 290.
Dickman, R. L. 1985, in *Protostars and Planets II*, ed. D. C. Black and M. S. Matthews (Tucson: University of Arizona Press), in press.
Kampé de Fériet, J. 1955, in *Gas Dynamics of Cosmic Clouds* (Amsterdam: North-Holland), p. 134.
Kaplan, S. A. and Klimishin, I. A. 1964, *Soviet Astr.—AJ*, **8**, 210.
Kleiner, S. C. 1985, Ph.D. thesis, University of Massachusetts.
Kleiner, S. C., and Dickman, R. L. 1984, *Ap. J.*, **286**, 255 (Paper I).
Kleiner, S. C. and Dickman, R. L. 1985*a*, *Ap. J.*, **295**, 466 (Paper II).
———. 1985*b*, in preparation (Paper IV).
Lumley, J. L. 1970, *Stochastic Tools in Turbulence* (New York: Academic).
Münch, G. 1958, *Rev. Mod. Phys.*, **30**, 1035.
Papoulis, A. 1965, *Probability, Random Variables and Stochastic Processes* (New York: McGraw-Hill).
Scalo, J. M. 1984, *Ap. J.*, **277**, 556.
———. 1985, in *Protostars and Planets II*, ed. D. C. Black and M. S. Matthews (Tucson: University of Arizona Press), in press.
Tatarskii, V. I. 1961, *Wave Propagation in a Turbulent Medium* (New York: McGraw-Hill).

ROBERT L. DICKMAN and STEVEN C. KLEINER: Radio Astronomy, Graduate Research Center, University of Massachusetts, Amherst, MA 01003